



**Design strategies of fluorescent probes for selective detection among biothiols**

Journal:	<i>Chemical Society Reviews</i>
Manuscript ID:	CS-REV-02-2015-000152.R1
Article Type:	Review Article
Date Submitted by the Author:	12-May-2015
Complete List of Authors:	Yang, Qing-Zheng; Technical Institute of Physics and Chemistry, CAS, Niu, Li-Ya; Technical Institute of Physics and Chemistry, Chen, Yu-Zhe; Technical Institute of Physics and Chemistry, CAS, Zheng, Hai-Rong; Technical Institute of Physics and Chemistry, Wu, Li-Zhu; Technical Institute of Physics and Chemistry, CAS, Tung, Chen-Ho; Technical Institute of Physics and Chemistry,

## ARTICLE

## Design strategies of fluorescent probes for selective detection among biothiols

Cite this: DOI: 10.1039/x0xx00000x

Li-Ya Niu,<sup>a,b</sup> Yu-Zhe Chen<sup>b</sup>, Hai-Rong Zheng,<sup>b</sup> Li-Zhu Wu<sup>b</sup>, Chen-Ho Tung<sup>b,c</sup> and Qing-Zheng Yang<sup>a,b</sup>

Received 00th January 2012,  
Accepted 00th January 2012

DOI: 10.1039/x0xx00000x

www.rsc.org/

Simple thiol derivatives, such as cysteine (Cys), homocysteine (Hcy), and glutathione (GSH), play key roles in biological processes and the fluorescent probes to detect such thiols in vivo selectively, with high sensitivity and fast response times are critical for understanding their numerous functions. Yet the similar structures and reactivities of these thiols pose considerable challenge to the development of such probes. This review focuses on various strategies for the design of fluorescent probes for selective detection of biothiols. We classify the fluorescent probes for the discrimination among biothiols according to reaction types between probes and thiols, such as cyclization with aldehydes, conjugate addition-cyclization with acrylates, native chemical ligation, and aromatic substitution-rearrangement.

### 1. Introduction

Biothiols, such as cysteine (Cys), homocysteine (Hcy) and glutathione (GSH) (Fig. 1), play many crucial roles in biological systems. The metabolism and transportation of these sulfur-containing compounds in biological systems are associated with a series of important enzymes and proteins. The endogenous concentrations of these thiols suggest the functional state of the corresponding enzymes and proteins, and their abnormal levels correlate with diseases. For example, an abnormal level of cysteine is implicated in liver damage, skin lesions, and slowed growth, *etc.*<sup>1</sup> Deficiency in the expression of enzymes such as cystathionine  $\beta$ -synthase and cystathionine  $\gamma$ -lyase or their cofactors may lead to abnormal accumulation of Hcy, which characterizes inherited diseases such as homocystinuria, and cardiovascular abnormalities.<sup>2</sup> GSH is the most abundant intracellular nonprotein thiol. The ratio of free GSH and its oxidized state glutathione disulfide (normally > 100:1) is an indicator for the corresponding enzyme activity and the redox state of the cell.<sup>3</sup> These examples illustrate the importance of the detection and monitoring of thiol-containing molecules in biological samples both for understanding the functionality of thiol-containing enzymes and proteins in physiological and pathological processes, and for potential use in clinical diagnosis.

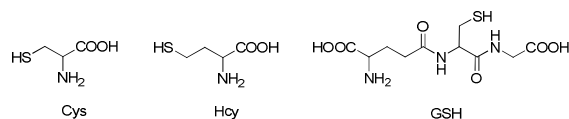


Fig. 1 Chemical structures of Cys, Hcy and GSH.

Fluorescent sensing is attractive for its potentially very high sensitivity and excellent temporal-spatial resolution and fairly simple technical implementation.<sup>4-7</sup> The interaction between analytes and fluorescent probes, which changes the probes spectroscopic characteristics, can either be based on reversible supramolecular (non-covalent) interactions, such as hydrogen bonding,  $\pi$ - $\pi$ , donor - acceptor, electrostatic, hydrophobic, hydrophilic, and coordination-based interactions, or on irreversible covalent interactions.<sup>8, 9</sup> The latter generally provide superior selectivity as a result of exploiting the specific covalent reactions that are less dependent than non-covalent systems on the complementarity between the host and the guest.<sup>10, 11</sup> For a reaction to be a suitable trigger for detection and imaging applications, it must proceed with suitable kinetics under biological constraints, to allow the detection of analytes present at low concentrations or that have short lifetimes. Thus the key chemical challenge in designing the probes is to identify reactions that combine fast rate, high chemoselectivity and bioorthogonality.<sup>12</sup>

In this review, we will summarize and analyse various strategies – some demonstrated, others only suggested – for the design of fluorescent probes for rapid, selective and quantitative detection of thiols. We will not cover the developments in the field previously reviewed,<sup>13-15</sup> but rather focus on methods that allow differentiation among biothiols of similar structures and reactivities, and attempt to offer a critical evaluation of the underlying principles with the hope that this may inform the future development and refinement of such methods.

## 2. Fluorescent probes for discrimination of biothiols

### 2.1 Fluorescent probes for selective detection of biothiols over other amino acids

Appropriately designed reaction-based probes have enabled the discrimination of thiols from other biological species. These probes were designed to exploit the strong nucleophilicity of the sulfhydryl group, which enables reactions such as Michael addition<sup>16, 17</sup>, cleavage of sulfonamide and sulfonate esters<sup>18, 19</sup>, cleavage of S-S bond<sup>20, 21</sup> or Se-N bond, etc.<sup>13</sup> In this section we will briefly introduce above reaction-based probes and give some typical examples.

Michael addition, known as the addition of a nucleophile to an  $\alpha,\beta$ -unsaturated carbonyl moiety, has been widely used as a basis of fluorescent probes for biothiols. The frequently used Michael acceptors include maleimide, squaraine, acrylamide derivatives, etc.

Michael addition to a maleimide group that recovers the fluorescence of the probe is exploited by probes **1**<sup>22</sup> and **2**<sup>23</sup> (Fig. 2). In these compounds, luminescence of BODIPY or Tb(III) complex is quenched by photoinduced electron transfer (PET) to maleimide. Upon addition of a thiol (forming **1-S** or **2-S**), the luminescence is recovered. Interestingly, efficient PET from BODIPY to maleimide was only observed in the ortho substituted derivative; the meta- and para substituted analogs of **1** were highly fluorescent [quantum yields of them are 0.37 (*meta*) and 0.54 (*para*) vs. 0.002 (*ortho*)]. Thus **1** responded to thiols with a high signal-to-noise ratio (350-fold difference in fluorescence of **1** vs. **1S**). The main advantage of the Tb(III)-based probe **2** for bioimaging is its narrow, long-wavelength emission and long-lived excited states, enabling probe luminescence to be distinguished from short-lived autofluorescence. Probe **2** was successfully employed to monitor the enzymatic conversion of oxidized form of glutathione (GSSG) to GSH in real time.

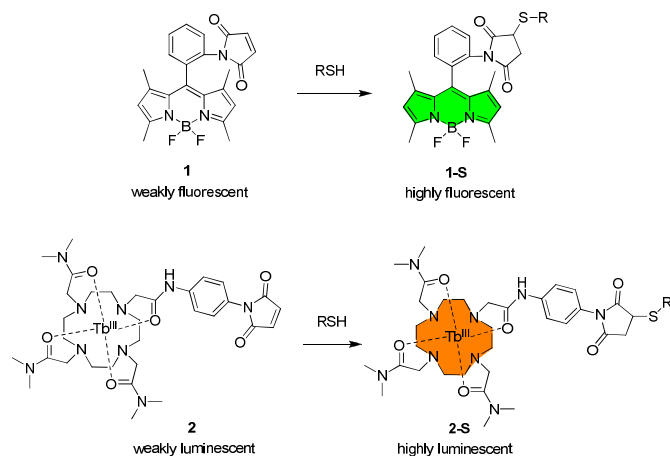


Fig. 2 Michael addition reaction of **1** and **2** with thiols.

The Ajayaghosh group reported a near infrared (NIR) fluorescent probe **3** based on a  $\pi$ -extended squaraine dye (Fig. 3)<sup>24</sup>. NIR spectroscopy is emerging as a very powerful tool in tissue imaging because light in the 650–900 nm range is known to penetrate deeper than visible light. Squaraines exhibit sharp and intense absorption (extinction coefficients  $\geq 10^5$  cm<sup>-1</sup> M<sup>-1</sup>) at long wavelengths (620–670 nm)<sup>25</sup>. This absorption and emission maximum was further shifted to NIR ( $\lambda_{\text{abs}} = 730$  nm,  $\lambda_{\text{em}} = 800$  nm) by derivatizing the squaraine with two  $\pi$ -bispyrroles to extend  $\pi$ -conjugation, in probe **3**. The addition of a thiol interrupted the  $\pi$ -conjugation, shifting the spectra from NIR to visible wavelengths ( $\lambda_{\text{abs}} = 440$  nm,  $\lambda_{\text{em}} = 592$  nm). The probe was used for estimating biothiol concentration in human blood plasma and confirmed that smoking increased the blood level of biothiols.

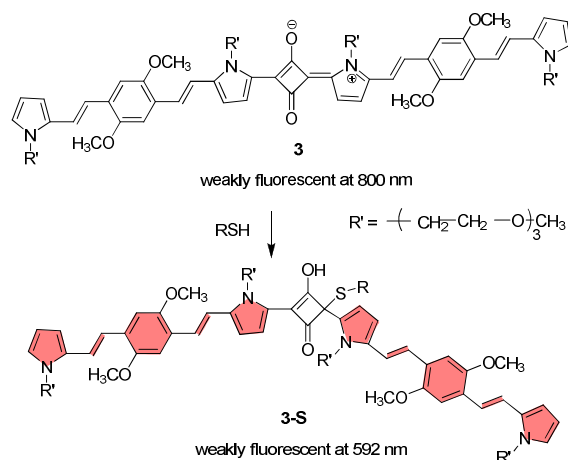


Fig. 3 Michael addition reaction of **3** with thiols.

The Xi group reported fluorescent probe **4** (Fig. 4) for an extraordinarily sensitive and fairly fast biothiol quantification: the adduct of **4** and thiol, **4-S**, is 470-fold more fluorescent than the probe.<sup>26</sup> The observed rate constant of pseudo-first-order reaction of **4** with Cys was  $2.4 \times 10^2$  s<sup>-1</sup> ( $t_{1/2} = 3$  ms). The reaction between **4** (10  $\mu\text{M}$ ) and 0.2 equiv of Cys was complete in less than a minute at room temperature in aqueous media (pH 7.4). Probe **4** was used to quantitatively label thiol-containing proteins, such as bovine serum albumin (BSA), at very low concentration (50 ng).

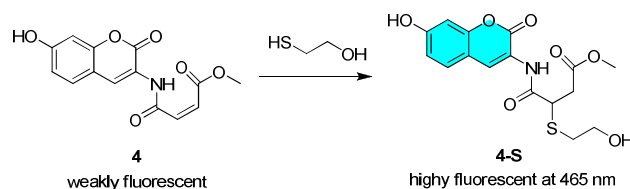


Fig. 4 Michael addition reaction of **4** with thiols.

Strongly electron-deficient 2,4-dinitrophenyl sulfonyl group serves as an efficient fluorescence quencher when attached to a fluorophore and can be displaced by strong nucleophiles. It was used to give probes **5**<sup>27</sup> and **6**<sup>28</sup>, which are non-fluorescent but undergo rapid irreversible S<sub>N</sub>Ar reaction in the presence of

thiols, yielding fluorescein or cresyl violet with high fluorescence (Fig. 5). Probe **5** was used for measuring acetyl- and butyryl-cholinesterase inhibitory activities, whereas probe **6** enabled quantitation and imaging of microsomal glutathione transferase (GST) activity in living cells (GSTs play an important role in cellular protection from environmental and oxidative stress, and are overexpressed in certain tumors).

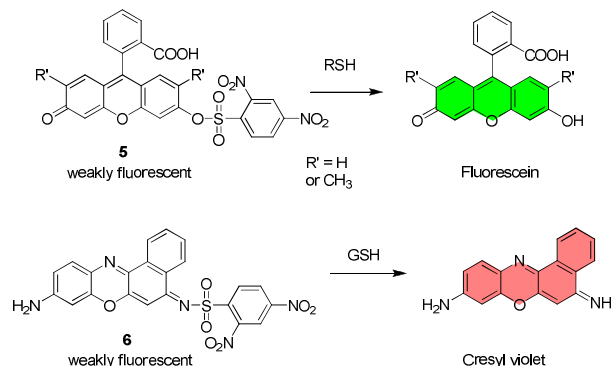


Fig. 5 Reaction of **5** and **6** with thiols to release the fluorescent products.

The Cho group reported a two-photon fluorescent probe **7** for the detection of thiols based on thiol/disulphide exchange (Fig. 6).<sup>29</sup> Two-photon microscopy, using two near infrared photons as the excitation source, has the advantages of high tissue penetration depth, localized excitation, and prolonged observation time, thereby allowing tissue imaging. Probe **7** was derived from 2-methylamino-6-acetylnaphthalene bearing a disulfide group as the thiol reaction site. Thiol/disulphide exchange, followed by intramolecular nucleophilic displacement yielded amino-acetylnaphthalene with two-photon fluorescence 10-times that of **7**. The probe enabled imaging in living cells and rat tissue at a depth of 90-180  $\mu\text{m}$ .

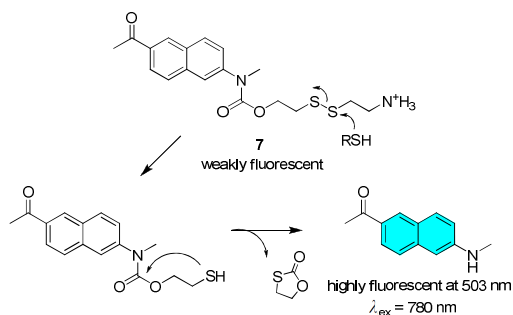


Fig. 6 The reaction between **7** and thiols based on thiol/disulphide exchange.

The same chemistry was exploited in probe **8** (Fig. 7),<sup>30</sup> designed for hepatic thiol imaging, ensured by the presence of the hepatocyte-targeting galactose moiety. The 473 nm emission maximum of probe **8** shifted to 540 nm in the presence of thiols. The fluorescence imaging in living rats confirmed that **8** accumulated selectively in the liver.

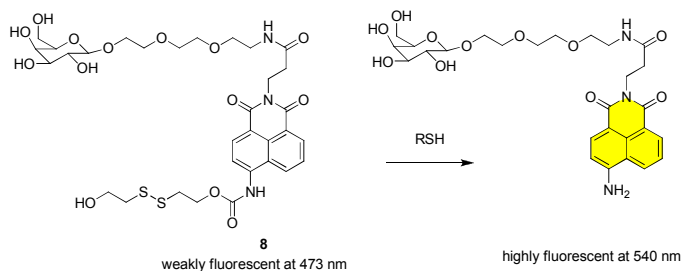


Fig. 7 Probe **8** bearing hepatocyte-targeting galactose moiety for detection of thiols.

The Tang group reported probes **9-10** based on the chemistry of the Se-N bond (Fig. 8). Irreversible reaction of non-fluorescent probe **9** with diverse thiols, including protein thiols such as thioredoxin, glutathione reductase, and metallothionein generated highly fluorescent rhodamine 6G.<sup>31</sup> Probe **10** was inspired by ebselen (2-phenyl-1,2-benzisoselenazol-3(2H)-one), an anti-inflammatory drug bearing a Se-N bond that catalyses the reduction of hydrogen peroxide in the presence of thiols. Ebselen was integrated with an NIR fluorophore, heptamethine cyanine, reacts with GSH/H<sub>2</sub>O<sub>2</sub> reversibly and is suitable for monitoring redox status in vivo.<sup>32</sup>

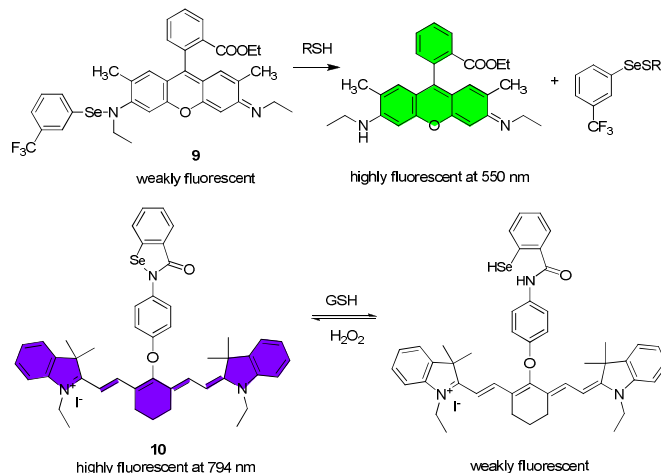


Fig. 8 The irreversible or reversible reaction of Probe **9** and **10** with Se-N bond.

## 2.2 Fluorescent probes for selective detection among biothiols

Although the detection of total biothiols is well developed, discrimination among biothiols remains a challenge. Such differentiation is of great biochemical interest given the diverse biological roles of different thiols. For example, the elevated levels of Hcy in plasma are associated with cardiovascular and Alzheimer's diseases, whereas abnormal levels of GSH correlate with heart problems, cancer, and aging.

The design principle for differentiating Cys and Hcy from other thiols is to exploit the synergistic effect of their sulfhydryl group and the adjacent amine group, which enables specific reactions, such as cyclization with aldehydes, conjugate

addition-cyclization with acrylates, native chemical ligation, and aromatic substitution-rearrangement.

### 2.2.1 Cyclization with aldehydes

The aldehydes react with the N-terminus of Cys to form thiazolidines, a reaction that is routinely used to label and immobilize peptides and proteins. The elaboration of cyclization between aldehydes and Cys/Hcy to yield thiazolidines/thiazinanes was utilized to construct fluorescent probes (Fig. 9), and it became the most frequently used reaction types for differentiating Cys/Hcy from GSH.<sup>33-38</sup>

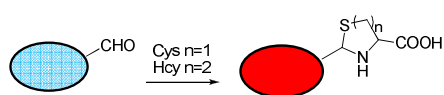


**Fig. 9** Schematic illustration of the reaction of aldehyde-bearing fluorophore with Cys/Hcy to yield thiazolidine/thiazinane.

It was exploited by the Strongin group in 2004 to create the first example of a probe (**11**) for the selective detection of the Cys/Hcy over GSH (Fig. 10).<sup>39</sup> The formation of thiazolidine/thiazinane between aldehyde and Cys/Hcy led to a 25 nm red shift in the absorption spectrum and a decrease in fluorescence intensity. Probe **11** was applied to detect Cys and Hcy in blood. The addition of Cys to a sample of human blood plasma containing **11** and excess GSH induced a red shift in absorption from 480 to 505 nm with the increasing concentration of Cys. The fluorescence intensity of plasma containing **11** showed a linear correlation with the Hcy concentrations over the range from healthy to abnormal level ( $2.9 \times 10^{-6}$  -  $2.5 \times 10^{-3}$  M).

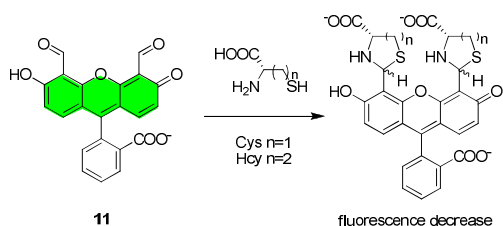


**Fig. 10** The cyclization reaction of **11** with Cys/Hcy.

The analyte-induced quenching of fluorescence of probe **11** was only observed at basic pH 9.5, potentially limiting their physiological application. Aldehyde-functionalized probes with fluorescence enhancement and ratiometric signals have received a great deal of attention. The Barbas group reported a turn-on fluorescent probe **12** for Cys detection over GSH (Fig. 11). The concentration of Cys in the range of 100  $\mu$ M - 5 mM was well correlated with the fluorescence intensity at 380 nm. Probe **13** displayed an emission band at 519 nm due to the intramolecular charge transfer (ICT) from the electron rich phenanthroimidazole core to the electron-deficiency aldehyde acceptor (Fig. 11)<sup>40</sup>. Upon addition of Cys/Hcy, **13** exhibited a large emission shift (125 nm) as a result of switching off ICT. The fluorescent intensity ratios ( $I_{394 \text{ nm}}/I_{519 \text{ nm}}$ ) showed a good

linear relationship with Cys concentrations ranging from 6 to 800  $\mu$ M.

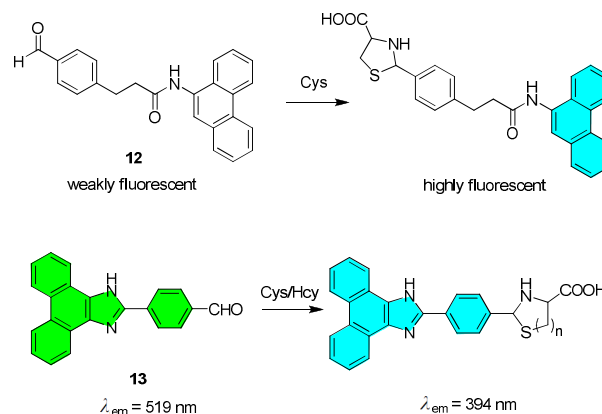


**Fig. 11** The cyclization of **12** and **13** with Cys/Hcy.

The generality of this strategy is further illustrated by selective detection of Cys/Hcy in the presence of other thiols and other biomolecules by probes based on coumarin (**14**)<sup>41</sup>, BODIPY (**15**)<sup>42</sup>, naphthalimide (**16**)<sup>43</sup> dyes, two-photon absorption dyes (**17**)<sup>44</sup>, and organometallic dyes (**18**)<sup>45</sup>, etc (Fig. 12).

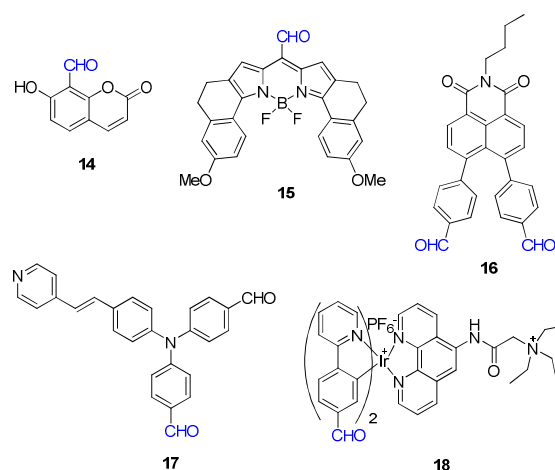


**Fig. 12** Chemical structures of probe **14-18** containing aldehyde group.

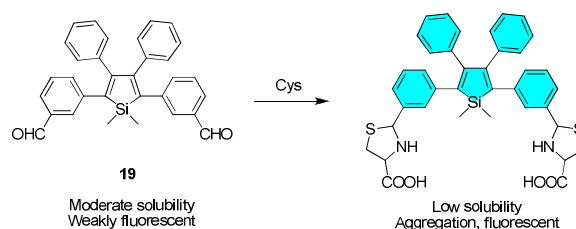


**Fig. 13** Mechanistic representation of **19** for detection of Cys.

Distinct from above is fluorescent probe **19**, which was based on the phenomenon of aggregation induced emission, AIE (Fig. 13).<sup>36</sup> AIE dyes become emissive only upon aggregation. In DMSO/HEPES buffer probe **19** is very weakly emissive at 479

nm. The intense AIE-emission band at 424 nm was observed upon the reaction with Cys, resulting from the aggregation of the weakly soluble product **19**-Cys. The order of the sensitivity of **19** for biothiols was Cys > Hcy > GSH.

Unlike most other aldehydes that react with Cys and Hcy at similar rates, cyclization with certain  $\alpha,\beta$ -unsaturated aldehydes allows selective detection of Cys over Hcy, as demonstrated by the Strongin group with commercially available cinnamaldehyde derivatives **20** in 2005 (Fig. 14)<sup>46</sup>. Cys reacted with **20** to form 5-membered ring heterocycles, whereas Hcy was essentially inert (only trace amounts of imine was observed). The least reactive electrophile **20c** exhibited the highest selectivity towards Cys. Addition of Cys to a solution of **20c** (pH 9.5) resulted in the disappearance the yellow color; while Hcy did not lead to any color change under the identical conditions.

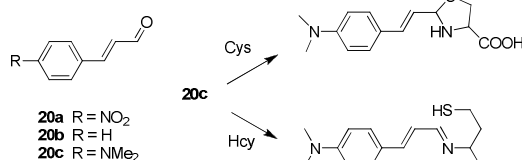


**Fig. 14** The chemical structures of **20a-c** and the reaction of **20c** with Cys and Hcy.

The strategy was further elaborated by the Peng group to develop fluorescent probe **21** that showed good selectivity towards Cys over Hcy (Fig. 15).<sup>47</sup> Probe **21** is colorless and weakly fluorescent in ethanol/PBS buffer (3:7 v/v, pH 7.0). Upon addition of Cys to **21**, an absorption band appeared at 531 nm, and the fluorescence intensity at 552 nm increased rapidly. The fluorescence intensity at 552 nm was linearly proportional to Cys concentrations with detection limit of  $7.35 \times 10^{-8}$  M. The reaction of Cys with **21** generated an unstable intermediate **21**-Cys, followed by ring-opening and hydrolysis to yield highly fluorescent rhodamine. By contrast, the reaction with Hcy produced stable colorless and non-fluorescent **21**-Hcy. Probe **21** was used to imaging exogenous Cys in living cells, and to quantify Cys in human urine.

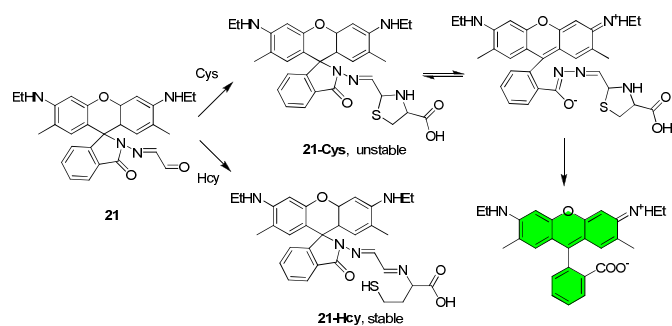


**Fig. 15** The reaction of **21** with Cys and Hcy for the selective detection of Cys over Hcy.

Ratiometric fluorescent probe **22**, based on coumarin dye bearing a  $\alpha,\beta$ -unsaturated aldehyde group, was reported for specific detection of Cys over Hcy and GSH (Fig. 16).<sup>48</sup> Probe **22** showed emission band at 557 nm in CH<sub>3</sub>CN/PBS buffer (v/v, 1:9, pH 7.4). Upon addition of Cys, a marked decrease of the fluorescence intensity at 557 nm was observed, accompanied by a dramatic fluorescence enhancement at 487 nm. The amino group of Cys initially reacted with aldehyde to afford the imine intermediate **22**-M1, which then underwent a ring closure to generate an intermediate **22**-M2 that further reacted with one more Cys to form **22**-Cys. In contrast, the emission ratio ( $I_{487\text{ nm}}/I_{557\text{ nm}}$ ) changed only little in the presence of Hcy and GSH. The rate constant for Cys was  $\sim 1000$ -fold and  $\sim 19000$ -fold faster than that for Hcy and GSH, respectively, which explained the high selectivity of **22** to Cys over Hcy and GSH. The  $\alpha,\beta$ -unsaturated aldehyde groups were also exploited in BODIPY (**23**)<sup>49</sup> and carbazole (**24**)<sup>50</sup> dyes to develop fluorescent probes for Cys (Fig. 17).

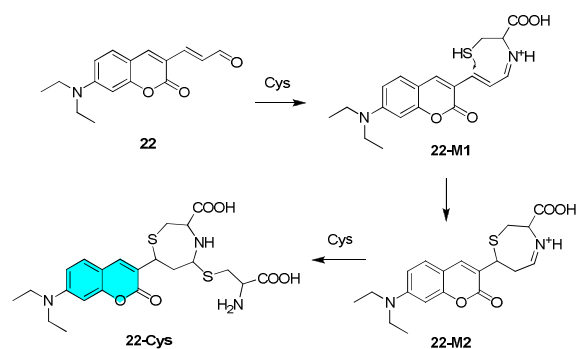


**Fig. 16** The reaction of **22** with Cys.

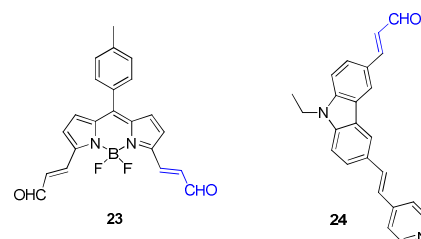


**Fig. 17** Chemical structures of **23** and **24**.

Selective detection of Hcy is a more challenging task than selective Cys detection: Only a few such probes have been reported.<sup>37, 46, 51-55</sup>

An example from the Li group was based on iridium(III) complex **25**.<sup>51</sup> Upon addition of Hcy to a solution of **25** in DMSO-HEPES buffer (9:1 v/v, pH 7.2), the emission at 525 nm increased significantly; by contrast, the addition of Cys did not induce emission enhancement. The luminescent quantum yield of **25**-Hcy was measured to be 0.038 and was remarkably higher than that of **25** ( $\sim 0.003$ ) and **25**-Cys ( $\sim 0.002$ ). Both surface charge analysis and electrochemical measurements indicated that thiazolidine is better electron donor than thiazinane resulting in efficient photoinduced electron-transfer

(PET) in 25-Cys and luminescent quenching, which was probably responsible for the high specificity of **25** toward Hcy over Cys. Similarly, the addition of Hcy to probe **26** led to the fluorescence enhancement at 450 nm, while Cys and other thiols did not manifest a significant fluorescence response.<sup>37</sup>

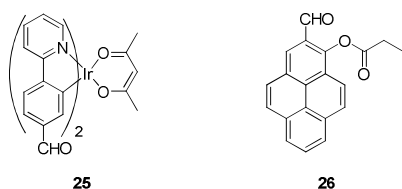


Fig. 18 Chemical structures of probe **25** and **26**.

Probe **27** exploited the slightly different basicity of the thiazolidine ( $pK_a \sim 5.7$ ) and thiazinane ( $pK_a \sim 6.7$ ) heterocycles formed by the reaction of **27** with Cys and Hcy, respectively and the capacity of the lone pair of amine groups to quench fluorescence by PET (Fig. 19).<sup>52</sup> In more acidic medium (pH 5.5), both thiols induced fluorescence from protonated derivatives **27H<sup>+</sup>**, whereas in more basic medium (pH 9.5) fluorescence was not observed in the presence of either Cys or Hcy. In pH 6.0, the more basic thiazinane of **27a** was protonated whereas the less basic thiazolidine analog was not. Consequently, in this pH only Hcy resulted in fluorescence. These investigations might be useful for guiding the fluorescence probes based on the cyclization of aldehyde for differentiation between Cys and Hcy.

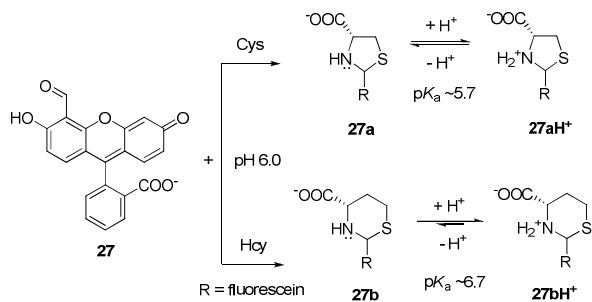


Fig. 19 Reactions of **27** with Cys and Hcy at pH 6.0.

In addition to the aldehyde-bearing probes, a selective colorimetric method for the detection of Hcy over Cys and GSH was described<sup>46, 53-55</sup> based on the generation of the Hcy thiyl radical by photolysis followed by the intramolecular hydrogen atom transfer (HAT) reaction to form  $\alpha$ -amino carbon centered radical. Such radical reduced methyl viologen ( $MV^{2+}$ ) or benzyl viologen ( $BV^{2+}$ ) to its corresponding radical cation (Fig. 20). This sensing mechanism of generating Hcy radical may inspire chemists to design fluorescent probes for differentiation of Hcy over Cys and GSH.

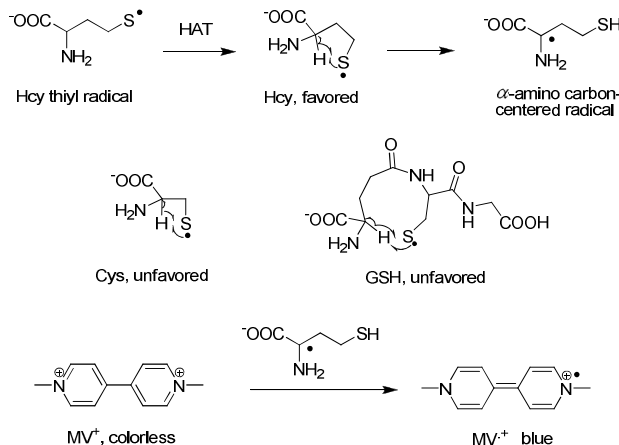


Fig. 20 Electron transfer from the Hcy carbon-centered radical to methyl viologen.

### 2.2.2 Conjugate addition-cyclization with acrylates

The Michael addition of Cys to acrylates initially generates thioethers which cyclize to 7-membered S,N heterocycles (1,4-thiazepane). This reaction has been used since 1966 in syntheses. In 2011 it was pioneered by the Strongin group, and then exploited extensively for detection of Cys and/or Hcy using acrylic esters of common fluorophores (such as fluorescein, and hydroxylated coumarins, naphthalimides and cyanines). In the presence of Cys, Hcy or GSH a thioether is formed by conjugated addition. With Cys and Hcy this is followed by cyclization with the release of free fluorophores, whereas with GSH the thioether is stable (Fig. 21). Differentiation between Cys and Hcy typically results from the much faster intramolecular cyclization of the Cys adducts compared to the Hcy analogs, which likely reflects the lower activation entropy for the formation of a 7- vs. 8-membered ring.

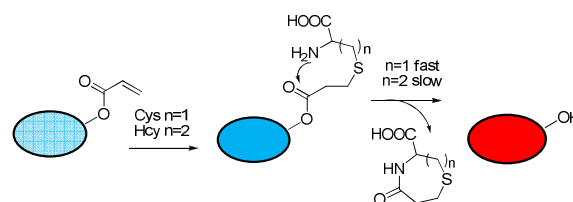
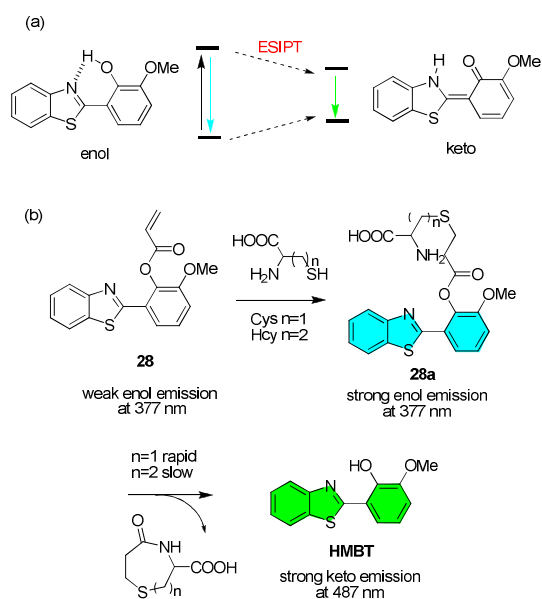


Fig. 21 Schematic illustration of the reaction of acrylic ester of fluorophore with Cys/Hcy through conjugated addition, followed by cyclization to yield free fluorophore.

Probe **28** and **29** were designed for the detection of Cys and Hcy by exploiting the phenomenon of excited-state intramolecular proton transfer (ESIPT)<sup>5</sup>. A typical ESIPT molecule 2-(2'-hydroxy-3'-methoxyphenyl) benzothiazole (**HBMT**) exhibits dual emission bands originating from its enol and keto tautomers (Fig. 22a). Probe **28** lacks ionizable protons does not participate in ESIPT and manifest a single weak enol emission band at 377 nm due to the alkene-induced PET quenching.<sup>56</sup> In thiol adducts **28a**, PET is eliminated, increasing

the emission intensity. The differences in the ring-formation kinetics to yield free **HMBT** with strong keto emission at 487 nm allowed the simultaneous detection of Cys and Hcy (Fig. 22b), whereas other amino acids cause no fluorescence intensity changes at 487 nm under the same conditions. The detection limits of Cys and Hcy are 0.11  $\mu\text{M}$  and 0.18  $\mu\text{M}$ , respectively. Similar phenomenon was observed in probe **29** (Fig. 23).<sup>57</sup> The reaction of Cys with **29** induced acrylate hydrolysis, thereby enabling ESIPT and shifting the weak blue emission (normal excited state, N\* emission at 380 nm) to a strong green emission (photo-tautomer, T\* emission at 510 nm) with  $\sim 20$ -fold enhancement. The potential of **28** for clinical applications was illustrated by demonstrating selective detection of Cys or Hcy in diluted deproteinized human plasma; probe **29** was used for fluorescent imaging of intracellular Cys.



**Fig. 22** (a) Schematic representation of ESIPT process of HMBT. (b) The reaction of **28** with Cys/Hcy.

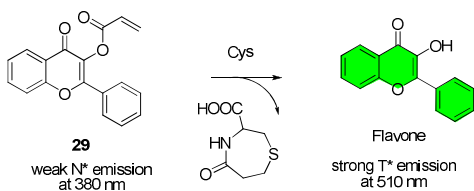


**Fig. 23** The reaction of **29** with Cys/Hcy.

The acrylation of fluorescein derivatives resulted in colorless and non-fluorescent spirocyclic molecules **30–32**, which allowed selective detection of Cys (Fig. 24). Upon addition of Cys, probes **30** and **31** underwent conjugated addition-cyclization to yield highly fluorescent fluorescein dyes ( $\lambda_{\text{abs}} = 478$  nm,  $\lambda_{\text{em}} = 515$  nm) by spirolactone-opening reaction.<sup>58</sup> Probe **30** showed better selectivity to Cys than **31**, probably resulting from the dual addition-cleavage processes for **30**. The detection limit of **30** for sensing Cys was evaluated to be 77 nM.

Probe **32** was constructed based on long-wavelength emitting seminaphthofluorescein. Both a pink color ( $\lambda_{\text{abs}} = 550$  nm) and strong fluorescence ( $\lambda_{\text{em}} = 621$  nm) were observed for probe **32** in the presence of Cys, whereas other amino acids and GSH cause almost no absorption and fluorescence changes.<sup>59</sup>

The masking of 7-hydroxycoumarin with acrylate yielded probe **33** that manifested weak fluorescence.<sup>60</sup> Its reaction with Cys released the highly fluorescent free coumarin dye with maximum emission at 456 nm (Fig. 25). The probe was used to detect Cys in calf serum and in living cells.

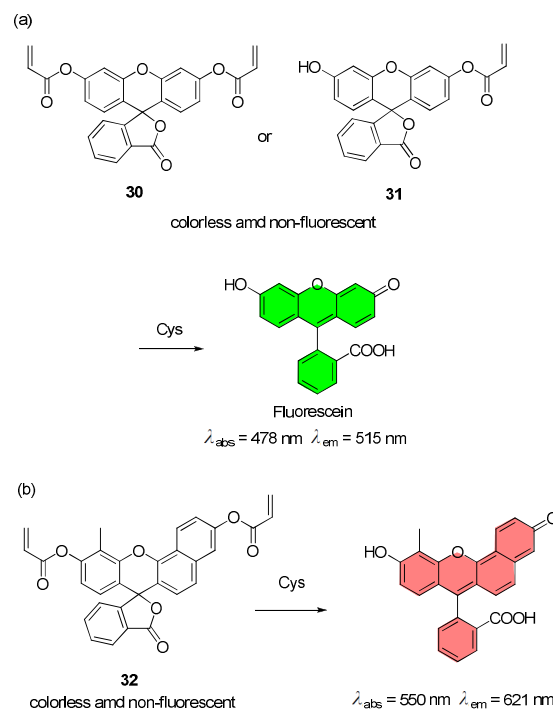


**Fig. 24** The reaction of **30–32** with Cys.

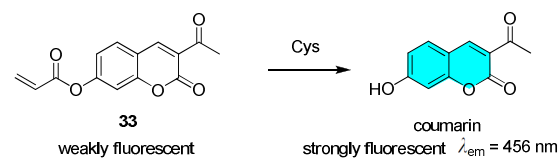


**Fig. 25** The reaction of **33** with Cys.

Unlike probes **28–33**, esters of 6-hydroxynaphthalimide (**34**)<sup>61</sup>, hydroxymercyanine (**35**)<sup>62</sup>, and hydroxycyanine (**36**)<sup>63</sup> are sufficiently emissive and have the absorption and emission maxima that are shifted to different extent relative to those of the free fluorophores, enabling both visual (“naked-eye”) and ratiometric detection of Cys (Fig. 26).

Absorption and emission bands of **34** are centered at 350 and 430 nm, respectively compared to 460 and 550 nm for hydroxynaphthalimide, which was released upon reaction of probe **34** with Cys in PBS buffer. Slightly smaller shifts in fluorescence maxima were reported for reaction of probe **35** with Cys in PBS buffer (pH 7.40): the absorption and emission maxima shifted from 384/488 nm to 512/552 nm. In these two

dyes, the shifts are due to the removal of electron-withdrawing acrylate group, which altered the “push–pull” character of the ICT fluorophores. The absorption and emission maxima of ester **36** are at 775 nm ( $\epsilon = 1.6 \times 10^5 \text{ M}^{-1} \text{ cm}^{-1}$ ) and 780 nm, respectively, whereas these maxima are at 515 and 520 nm in hydroxy-cyanine. The reason of such large shift is the keto-enol tautomerization upon Cys-triggered deesterification. Because of the very slow intramolecular cyclization of Hcy and GSH adducts of **36**, the probe was highly selective to Cys. The ratio of fluorescence intensities at 560 and 740 nm ( $I_{560 \text{ nm}} / I_{740 \text{ nm}}$ ) increased linearly with the Cys concentration from 0 to 25  $\mu\text{M}$ . Ratiometric imaging of Cys in MCF-7 cells with probe **36** was demonstrated. Those probes (**29-36**) were highly selective to Cys because the very slow intramolecular cyclization of the Hcy and GSH adducts did not generate any free fluorophores on the timescale of the measurements.

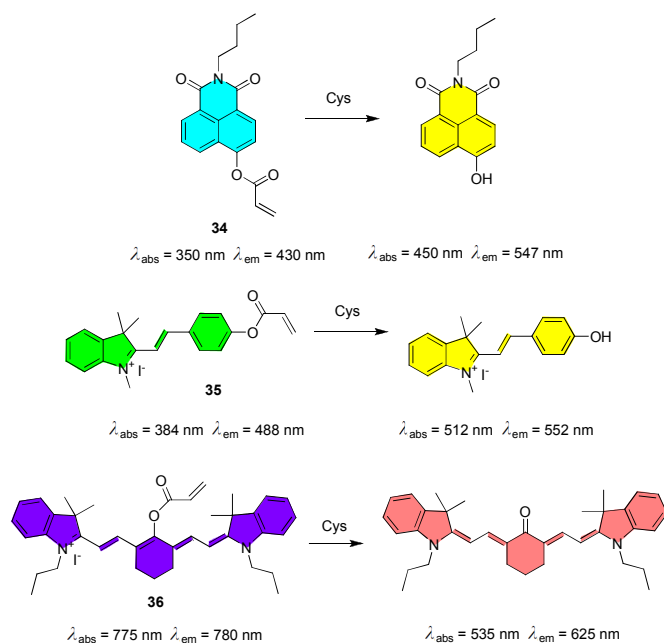


**Fig. 26** Ratiometric probe **34-36** for the detection of Cys.

The implementation of the masked fluorophore strategy using chloroacetate (**37**)<sup>64</sup>, bromoacetate<sup>65</sup> or chloropropionate<sup>66</sup> instead of acrylate as the thiol reactive masking group was demonstrated. In these Probes first the halide is displaced by Cys or Hcy, followed by cyclization releasing free fluorophore (Fig. 27).

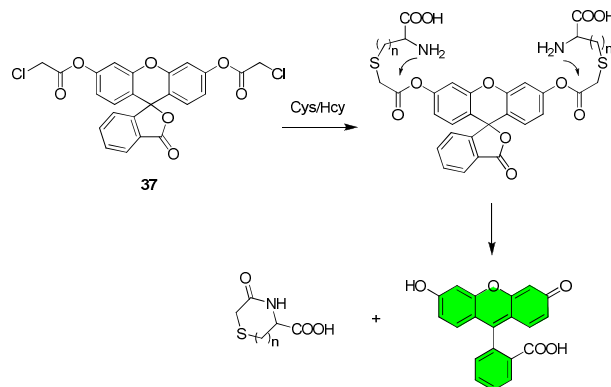


**Fig. 27** Probe **37** bearing a chloroacetate instead of acrylate for the detection of Cys/Hcy.

In an interesting departure from the pattern described above, probes **38-40** showed different selectivities towards thiols (Fig. 28). Probe **38** reacted with GSH to yield a fluorescent product, whereas Cys and Hcy gave non-fluorescent phenol derivatives,<sup>67</sup> enabling selective detection of GSH over Cys/Hcy. Surprisingly, acrylate ester **39** reacts with Cys, Hcy and GSH at approximately the same rate.<sup>68</sup> The puzzling lack of selectivity may be related to the probe's unusually high reactivity to thiols with a noticeable increase in fluorescence intensity in the presence of only 0.5  $\mu\text{M}$  concentrations of Cys. Probe **40** was exploited for selective detection of GSH in the CTAB (cetyltrimethylammonium bromide) media.<sup>69</sup> As expected, probe **40** showed good selectivity towards Cys in buffer solution. In order to achieve the selectivity of GSH over Cys/Hcy, CTAB micelles were introduced to catalyze the intramolecular closure of large rings, reversing the expected kinetics trend based on the ring size.<sup>70</sup> Other examples of surfactant-assisted fluorescent probes for GSH were also reported.<sup>71, 72</sup>

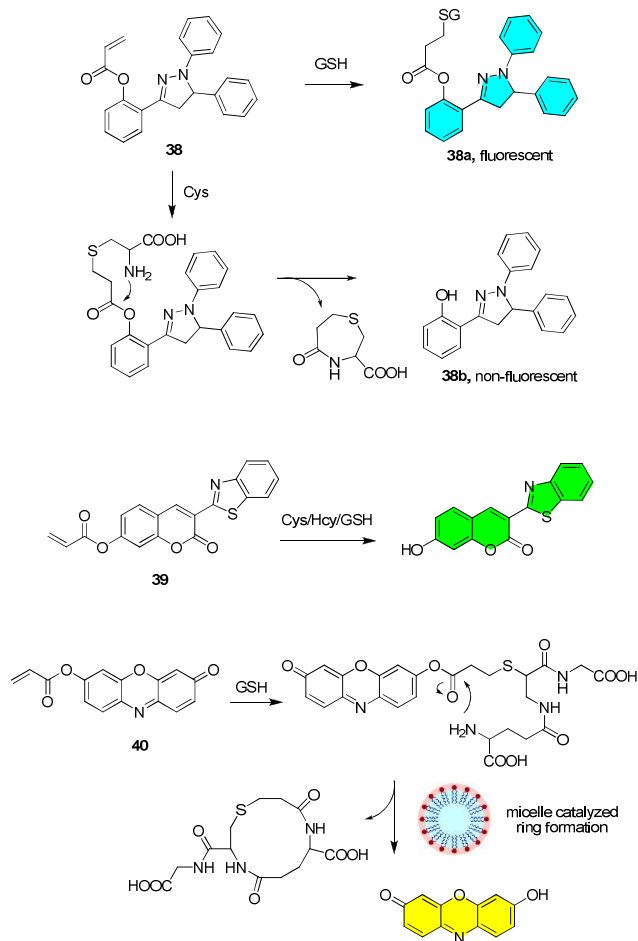


Fig. 28 The reaction of 38–40 with thiols.

### 2.2.3 Native chemical ligation

Native chemical ligation (NCL) is an important and powerful tool widely used for synthesis of proteins. Classical NCL is a reaction cascade starting with *trans*-thioesterification of a thioester at a C-terminus of a peptide by an N-terminal Cys residue of another peptide. The resulting thioester-linked intermediate undergoes an irreversible intramolecular *S,N*-acyl shift that forms a native amide bond at the ligation site. The above sequence is fast due to the proximity of the amino group to the thioester and the involvement of the five-membered intramolecular transition state (Fig. 29).

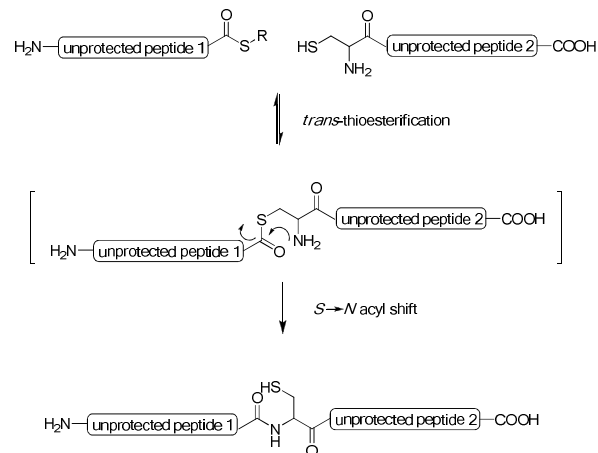


Fig. 29 Schematic illustration of the reaction mechanism of NCL.

Thioester of xanthene dyes have two important advantages for fluorescent detection of Cys/Hcy by NCL: (1) their thioester groups are highly reactive to transesterification by Cys/Hcy (2) the amide formation generates colorless and non-fluorescent spirocycles. However, it is not an optimal choice to directly employ thioester of xanthene dyes for sensing Cys/Hcy, because the generation of non-fluorescent spirocycles gives on-off fluorescent signals (Fig. 30). A preferable alternative is constructing ratiometric probes through integrating xanthene dye (or its analogue) into a Förster resonance energy transfer (FRET) pair (41, 42) or a large  $\pi$ -conjugated system (43, 44).

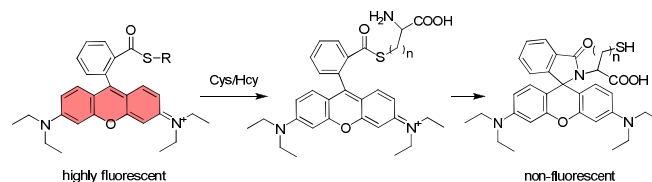


Fig. 30 Schematic illustration of the NCL reaction based on rhodamine platform.

Ratiometric fluorescent probes 41<sup>73</sup> and 42<sup>74</sup> were designed by the Lin group to exploit NCL-based FRET detection strategy (Fig. 31). The BODIPY donor was bridged to a rhodamine acceptor by a thioester linker that also served as the reaction site. The BODIPY donor was released in the presence of all of biothiols, making 41 a non-selective probe of biothiols.

In contrast, the FRET pair in probe 42 was connected by an inert short and rigid piperazine linker to ensure efficient FRET. Upon excitation at 395 nm, FRET dyad 42 emitted at 603 nm from the rhodamine acceptor. Treatment of 42 with Cys produced spirocyclic rhodamine 42a incapable of FRET, and resulted in fluorescence of the energy donor at 458 nm; a similar sensing behavior was also observed for Hcy. The measured rate constants ( $k_{\text{obs}}$ ) were 0.419  $\text{min}^{-1}$  for Cys and 0.335  $\text{min}^{-1}$  for Hcy under pseudo-first-order kinetic conditions. Almost no changes in the emission were observed in the presence of GSH, which generated thioester 42b without further intramolecular rearrangement. The emission ratios ( $I_{458 \text{ nm}}/I_{603 \text{ nm}}$ ) were proportional to the concentrations of Cys (1–100  $\mu\text{M}$ ) with a

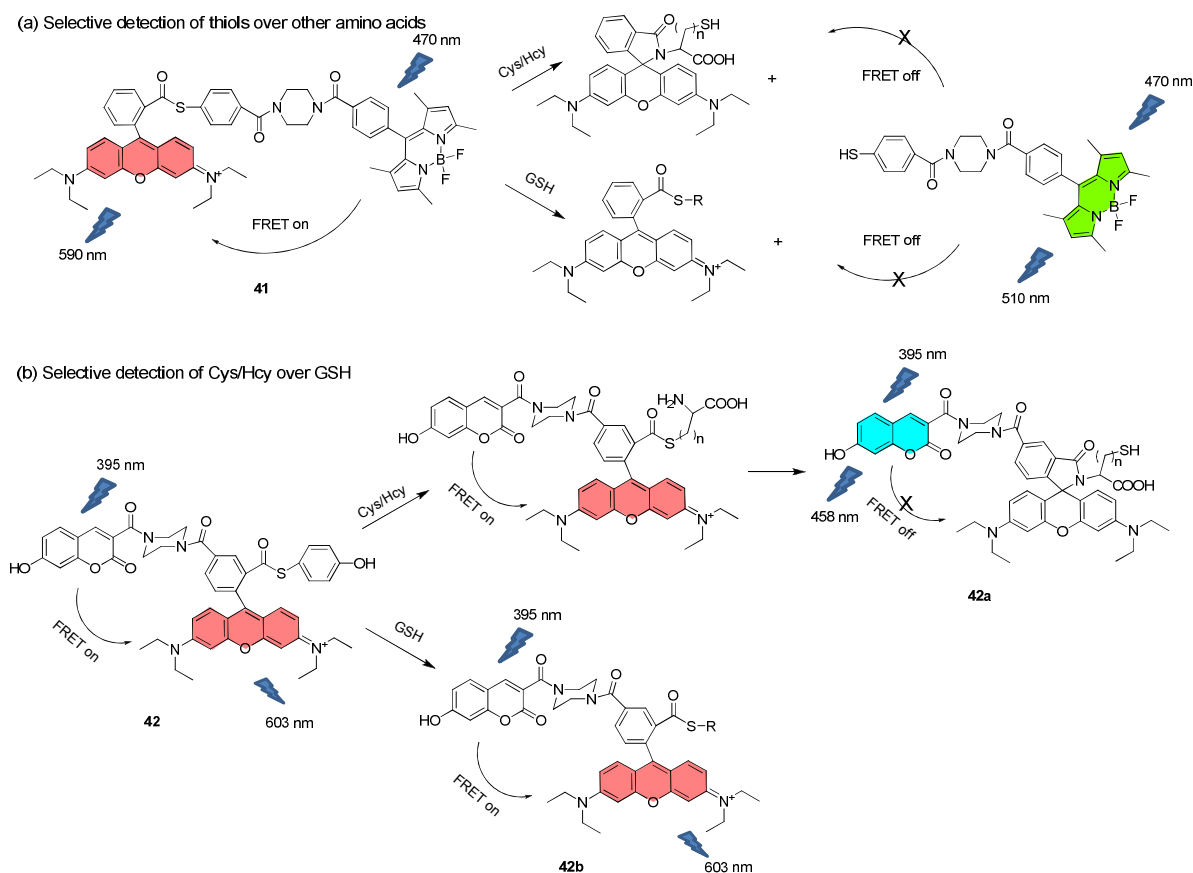


Fig. 31 FRET dyad **41** and **42** for the detection of thiols.

detection limit of  $6.4 \times 10^{-7}$  M, even in the presence of 1 mM GSH. Probe **42** was used to detect aminothiols in newborn calf and human serum samples and for ratiometric fluorescent imaging of Cys in living HepG2 cells.

Ratiometric fluorescent probe **43** exploited a hybrid NIR fluorophore of coumarin and benzopyrylium (Fig. 32). A fused phenyl thioester group served as the recognition group, thanks to its rapid NCL reaction than alkyl thioesters.<sup>75</sup> Upon addition of Cys to the solution of **43** in ethanol/phosphate buffer (40:60, v/v, pH 7.4), the original absorption band of **43** at 669 nm gradually decreased, with a concomitant increase in a new absorption band at 423 nm, resulting from interruption of the  $\pi$ -conjugation system. The solution color changed from dark blue to yellow-green, enabling a “naked-eye” detection of Cys. The fluorescence band at 694 nm decreased with concomitant growth of new emission band at 474 nm (coumarin emission). The distinct emission gap up to 220 nm facilitated the ratiometric sensing of Cys/Hcy. GSH only caused the thiol-thioester exchange, resulting in no change in fluorescence. Only very limited spectral changes were observed in the presence of other biologically relevant species (amino acids, metal ions). Probe **43** was applied as a ratiometric fluorescent probe for bioimaging of Cys/Hcy in living HepG2 cells.

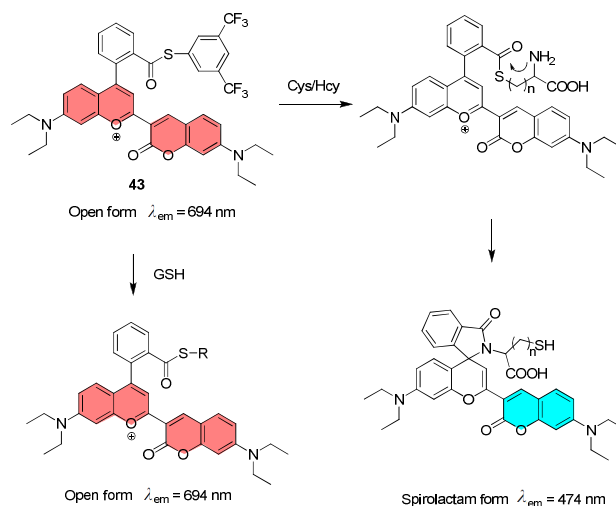


Fig. 32 Probe **43** for the detection of Cys/Hcy over GSH.

Yang et al reported dual-emission fluorescent probe **44** by exploiting both ESIPT and PET (Fig. 33).<sup>76</sup> They introduced a benzothiazole unit adjacent to the phenolic oxygen in the xanthene dye, thus facilitating the manipulation of ESIPT process within the molecule. In addition, the nitrothiophenol group served both as the

leaving group, and as a fluorescence quencher by PET process. Upon addition of biothiols to **44**, the weak fluorescence at 587 nm (rhodol emission) was turned on. Cys/Hcy further induced spirocyclization to give **44a**, and the resulting free phenolic group induced ESIPT, generating a new emission band at 454 nm from 2-(2-hydroxyphenyl)-benzothiazole (HBT). The probe was applied for the selective sensing of GSH and Cys in human breast cancer cells and reduced human serum. Dual-channel imaging of intracellular Cys and GSH was also demonstrated.

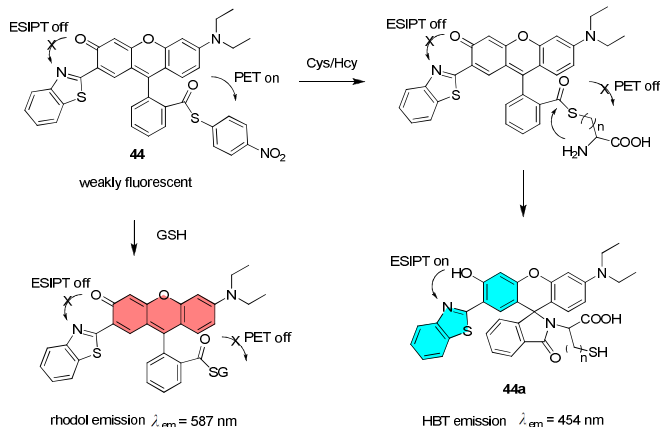


Fig. 33 Probe **44** for the simultaneous detection of Cys/Hcy and GSH.

### 2.2.4 Aromatic substitution-rearrangement reaction

Most examples using the above-mentioned reaction types were selective detection of Cys and/or Hcy over GSH. A strategy for the discrimination of GSH over Cys/Hcy was proposed by our group based on aromatic substitution-rearrangement cascade reaction (Fig. 34).<sup>77</sup> A fluorophore bearing a labile substituent reacts with thiols to yield thioether by nucleophilic aromatic substitution ( $S_NAr$ ). The amino groups of Cys/Hcy but not GSH further displace sulfur through a 5- or 6-membered transition states to yield the amino derivatives. The distinct photophysical properties of thioether- and amino- substituted dyes enable selective detection of GSH, Cys and/or Hcy.

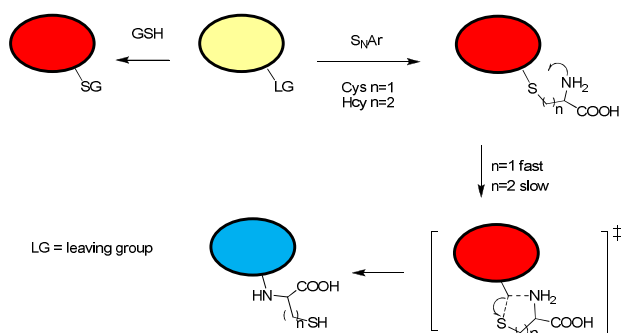


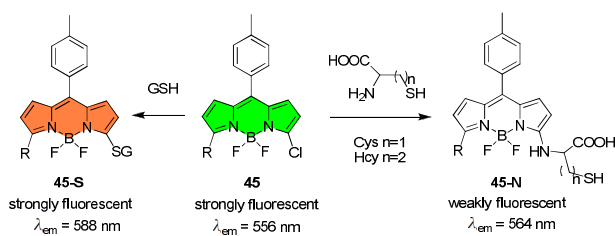
Fig. 34 Schematic illustration of the substitution-rearrangement cascade reaction.

A suitable fluorophore is the key element for constructing such a selective probe, and at a minimum it should (1) carry a reactive

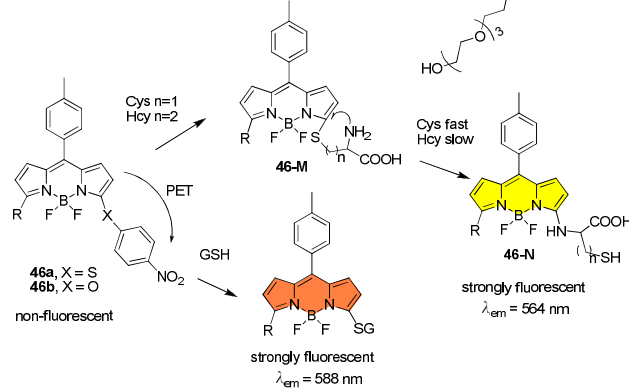
electrophilic site to enable its response to biothiols; and (2) manifest photophysical properties sufficiently distinct from those of the products of its reaction with the thiols.

Our BODIPY-based fluorescent probes **45–47** were carefully designed to meet these criteria (Fig. 35). Probe **45** showed an emission band centred at 556 nm in acetonitrile/HEPES buffer (5:95 v/v, pH 7.4).<sup>77</sup> Its Reaction with GSH generated thioether **45-S** with the maximum emission at 588 nm. The ratio of fluorescence intensities at the emission maxima of the product (**45-S**) and probe **45** ( $I_{588\text{ nm}}/I_{556\text{ nm}}$ ) was proportional to the GSH concentrations (0–60  $\mu\text{M}$ ), with the detection limit of  $8.6 \times 10^{-8}\text{ M}$ . In contrast, probe **45** reacted with Cys/Hcy to yield amines **45-N** with weak fluorescence at 564 nm, allowing it to be used for ratiometric detection of GSH over Cys/Hcy in living cells.

(a) Selective detection of GSH over Cys/Hcy



(b) Selective detection of Cys over Hcy/GSH



(c) Simultaneous detection of Cys/Hcy and GSH

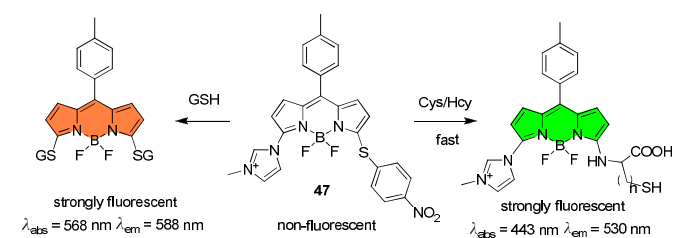


Fig. 35 BODIPY-based fluorescent probes **45–47** for the selective detection of biothiols.

Fluorescence of the amines was taken advantage for the detection of Cys by replacing the Cl substituent of **45** with nitrophenol or nitrothiophenol moieties (**46**, **47**), which suppressed fluorescence of the BODIPY core through PET. The addition of Cys to **46** yielded **46-N** through fast substitution rearrangement due to the favored

5-membered transition state and turned on the fluorescence. However, the intramolecular replacement reaction for Hcy took much longer time than Cys because it went through an unfavored 6-membered transition state. It enabled the discrimination of Cys from Hcy and GSH. Probe **47** was designed by attaching an electron-withdrawing imidazolium group to BODIPY core to increase the reactivity of nucleophilic aromatic substitution.<sup>78</sup> The emission intensities reached their maximum within 5 seconds and 2 minutes for Cys and Hcy, respectively, revealing the high reactivity of probe **47**. GSH replaced both the imidazolium and nitrothiophenol groups of **47** yielding dithioether with emission maximum at 588 nm. The simultaneous detection of GSH and Cys/Hcy was achieved by excitation at different wavelengths of 443 nm and 568 nm.

The same chemistry was exploited by Zhao and Ahn group to design BODIPY based probes **48**<sup>79</sup> and **49**<sup>80</sup> which were used for selective bioimaging of biothiols in living cells and in living zebrafish (Fig. 36).

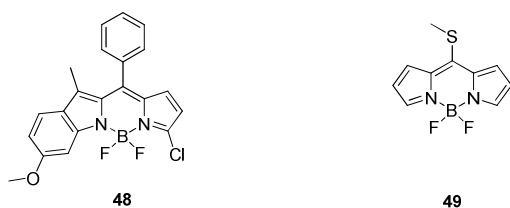


Fig. 36 Chemical structures of probe **48** and **49**.

In addition to BODIPY dyes, fluorophores such as nitrobenzofurazan (**50**), cyanine (**51**, **52**), naphthalimide (**53**, **54**), pyronin (**55**), were exploited as fluorescent probes for selective detection of thiols using same chemistry. These fluorescent probes were derived by modifications of two commercially available dyes, 7-nitro-2,1,3-benzoxadiazole (NBD-Cl) and heptamethine cyanine (IR-780), which themselves are useful for selective detection of biothiols.<sup>81</sup>

The ratiometric fluorescent probe **50** was designed for the detection of Cys/Hcy and H<sub>2</sub>S by a dual-fluorophore fragmentation strategy (Fig. 37).<sup>82</sup> Two fluorophores, nitrobenzofurazan (NBD) and coumarin were covalently linked. Cys/Hcy or H<sub>2</sub>S cleaved the adduct, generating coumarin ( $\lambda_{em} = 449$  nm) and NBD derivatives whose emission maxima depended on the thiol. Cys/Hcy generated **50a** with fluorescence at 549 nm, whereas H<sub>2</sub>S produced non-fluorescent **50b**. Coumarin acted as an internal standard, allowing the ratiometric measurement of **50a** versus **50b**, and thus the estimates of the concentration of Cys/Hcy or H<sub>2</sub>S. Treatment of **50** with GSH released the coumarin fluorophore and generated S-bound NBD, which was essentially nonfluorescent, and no fluorescence enhancement at 549 nm was observed. However, high levels of GSH would likely interfere with the ability of **50** to effectively differentiate H<sub>2</sub>S and Cys/Hcy in living cells.

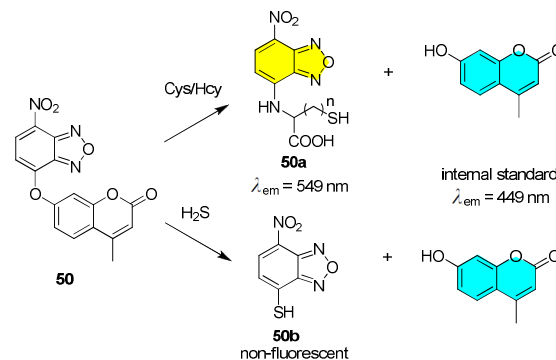


Fig. 37 Probe **50** for detection of Cys/Hcy and H<sub>2</sub>S with an internal standard.

Selective detection of GSH and Cys was demonstrated with Nitrophenyl substituted NIR probes **51**, **52** (Fig. 38).<sup>83, 84</sup> The substitution position or linking atoms in **51** was evaluated to have effect on the PET and fluorescence quantum yields. Probe **51a** with strongest PET effect was used to simultaneously detect GSH and Cys. Fluorescent probe **52** containing a tunable lipophilic cation unit as the biomarker for mitochondria was used for the detection of mitochondrial GSH in living cells.<sup>85</sup> The nitroazo ether group of **52** served both as a fluorescent quencher and as a leaving group. The weak fluorescence of **52** was likely to increase the S/N ratio for cellular imaging. Probe **52** may be applicable as a mitochondrial GSH tracker superior to the commercially available MitoTracker rhodamine 123 (Fig. 38).

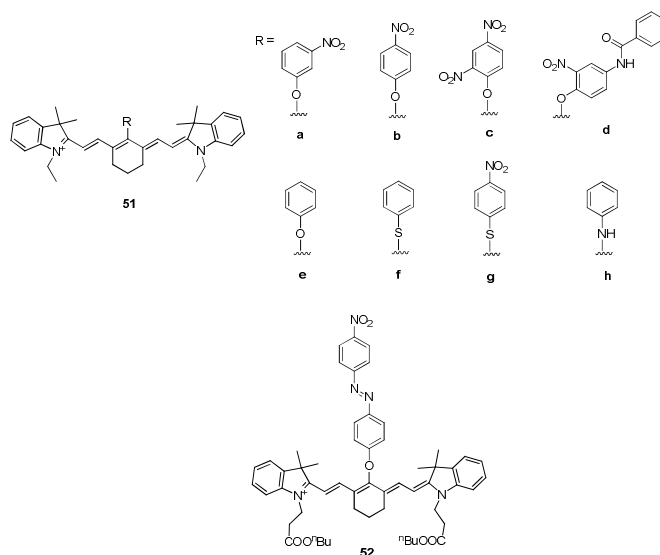
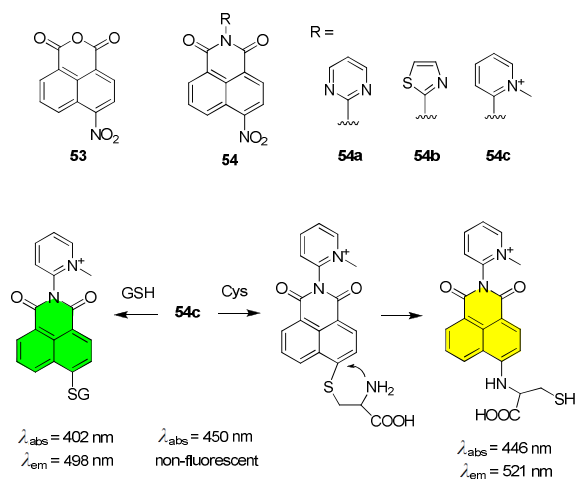


Fig. 38 Chemical structures of **51** and **52**.

Zhang and co-worker reported a series of fluorescent probes based on nitro-naphthalimide derivatives (Fig. 39). In their early work, probe **53** was employed to detect Cys, but only at 50 ° C and in DMF because of the low reactivity of **53**, which precluded its use in biological systems.<sup>86</sup> To improve the detection kinetics, they designed probes **54a-c** based on naphthalimide bearing electron-withdrawing heterocycles.<sup>87</sup> The most active probe, **54c** discriminated between GSH and Cys: **54c** reacted with GSH to

generate a highly fluorescent thioether ( $\lambda_{em} = 498$  nm,  $\lambda_{abs} = 402$  nm), with the fluorescence intensity at 498 nm linearly proportional to GSH concentrations in the range of 0–20  $\mu$ M, and the detection limit was  $5 \times 10^{-8}$  M. In the case of Cys, the amino product ( $\lambda_{em} = 521$  nm,  $\lambda_{abs} = 446$  nm) was only weakly fluorescent. The absorbances ratio at  $A_{446\text{ nm}}/A_{350\text{ nm}}$  increased linearly with the Cys concentration in the range of 0–70  $\mu$ M with detection limit of  $2 \times 10^{-7}$  M. It allowed the discrimination between Cys and GSH from different emissions at 521 nm and 498 nm.



**Fig. 39** Chemical structures of **53** and **54**, and the reaction of **54c** with Cys and GSH.

The methoxythiophenol moiety of probe **55** effectively quenches fluorescence of the pyronin core by PET is displaced by thiols leading to fluorescence enhancement at 546 nm (for Cys/Hcy) or 622 nm (for GSH, Fig. 40).<sup>88</sup> The maximum emission intensity was achieved in 2 min and 10 min in the presence of 15 equiv of GSH and Cys/Hcy, respectively. Probe **55** was used for simultaneous multicolor imaging of Cys/Hcy and GSH in living cells.

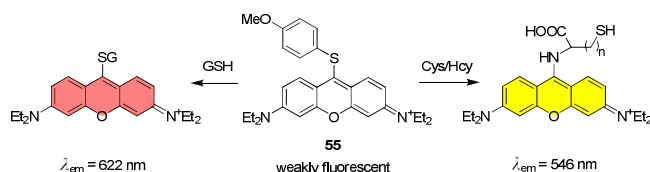


**Fig. 40** Detection of Cys/Hcy and GSH by Pyronin-based probe **55**.

Fluorescent probe **56** with three potential reaction sites was exploited to selectively detect Cys and Hcy by further elaboration of this strategy (Fig. 41).<sup>89</sup> Cys/Hcy replaced the chloro group (reaction site 1) of **56** to afford **56-M1**, which then cyclized to thiols **56-M2**. The thiol derived from Cys underwent rapid addition to the Michael receptor (site 2) yielding highly fluorescent amino-coumarin **56-Cys**. The same reaction was negligibly slow in the Hcy derivative, presumably due to higher energy of an 8-member cyclic transition state, relative to the 7-member analog in the Cys case. GSH also could replace the chlorine of **56** yielding **56-M3** which subsequently underwent macrocyclization at reaction site 3 to the final 14-membered ring product **56-GSH**. The distinct chemical structures

and spectral properties of **56-Cys** ( $\lambda_{abs} = 360$  nm,  $\lambda_{em} = 420$  nm), **56-M2** ( $\lambda_{abs} = 500$  nm,  $\lambda_{em} = 545$  nm) and **56-GSH** ( $\lambda_{abs} = 450$  nm,  $\lambda_{em} = 512$  nm) allowed the discrimination among Cys, Hcy and GSH. Probe **56** was used to simultaneously imaging Cys and GSH in living cell from different emission channels.

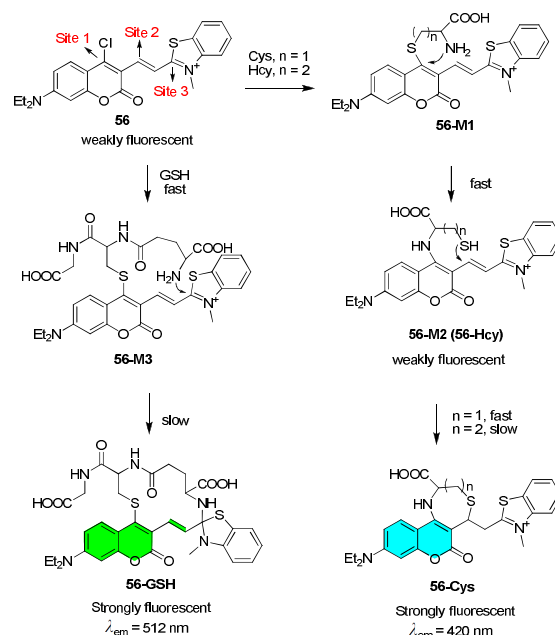


**Fig. 41** Probe **56** with three reaction sites for the detection of Cys, Hcy and GSH.

## 2.2.5 Other strategies

Supramolecular interactions, such as hydrogen bonding and electrostatic interaction are commonly used strategy to construct fluorescent probe. Yang et al developed a series of probes for selective detection of biothiols<sup>90-92</sup> based on classic spiropyran molecules that isomerize reversibly upon complementary electrostatic interactions with biothiols. Selective detection of GSH was demonstrated with bis-spiropyran **57** (Fig. 42),<sup>91</sup> which in the presence of GSH underwent ring opening to merocyanine with red-shifted emission band at 643 nm. Other thiols, including Hcy and Cys didn't induce isomerization of **57** probably because their size and/or charge distribution was less suited for strong binding to merocyanine. Probe **57** permeated cell membranes well, enabling its use for GSH imaging in living cells. However, probes that rely only on reversible non-covalent interactions tend to display moderate selectivity over other competitive species and are susceptible to interference in complex biological environments.

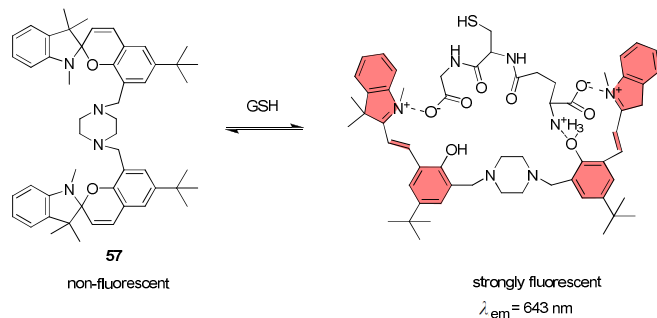


Fig. 42 Ring-opening of bis-spiropyran **57** for the detection of GSH.

Supramolecular interaction (e.g. electrostatic reaction, hydrogen bond) may also accelerate the specific reaction between biothiols and the probes, and thus improve the selectivity to certain thiols. As discussed in section 2.1, thiols add to Michael acceptors with little selectivity. By combining Michael addition with electrostatic attraction, fluorescent probe **58** displayed high selectivity for Cys (Fig. 43).<sup>93</sup> Probe **58** is almost non-fluorescent in PBS buffer due to the ICT process from the electron-donating diethylamino group to the electron-deficient pyridinium moiety. Upon addition of Cys, a 148-fold fluorescence enhancement at 500 nm was observed. By contrast, the addition of Hcy and GSH resulted in only 13 and 9-fold enhancements, respectively. The kinetic analysis revealed that **58** reacted with Cys 115-fold faster than with Hcy, and 36-fold faster than with GSH. The selectivity was attributed to electrostatic interactions between the cationic probe and negatively charged Cys. The isomers of **58**, **58'** was synthesized for evaluating the spatial influence of electrostatic interaction.<sup>94</sup> Cys adducts of **58'** underwent rapid cyclization to a non-fluorescent thiazepine derivative, presumably due to destabilization of the zwitterionic form. The results indicated that the proper spatial electrostatic interaction played a significant role in the selectivity and kinetics during the sensing process. Probe **58** displayed satisfactory cell permeability and was employed to imaging Cys in living cells.

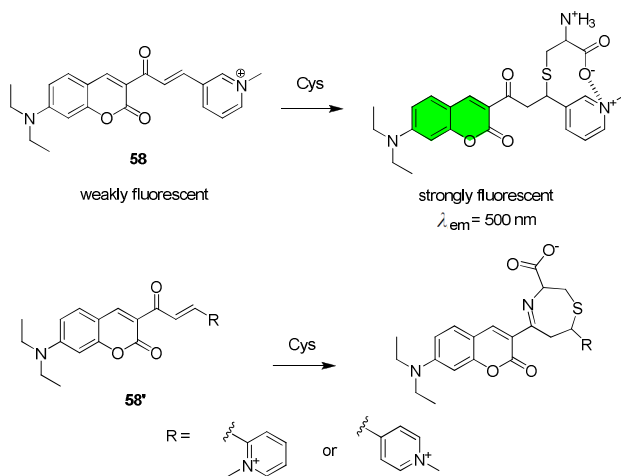


Fig. 43 The reaction of **58** and **58'** with Cys.

Fluorescent probe **59** showed high selectivity for Cys over Hcy using the similar chemistry to **58** (Fig. 44).<sup>95</sup> The emission intensity

of **59** at 644 nm decreased upon its reaction with Cys, while fluorescence at 494 nm increased gradually. The ratio of fluorescence intensities at the two wavelengths ( $I_{494\text{ nm}}/I_{644\text{ nm}}$ ) was enhanced 96-fold in the product relative to **59**. By contrast, the addition of Hcy and GSH increased the ratiometric value only 1.6 and 0.78-fold, respectively. Cys was expected to undergo NCL (native chemical ligation) reaction with **59** to produce intermediate **59-M1**, followed by intramolecular cyclization reaction to generate cyclic **59-Cys**. However, the reaction of **59** and Hcy resulted in thioester **59-Hcy**, which was attributed to an electrostatic attraction between cationic hemicyanine and negatively charged Cys that inhibited the subsequent *S,N*-acyl shift (See Fig. 44). Probe **59** was utilized to selectively image Cys in living cells.

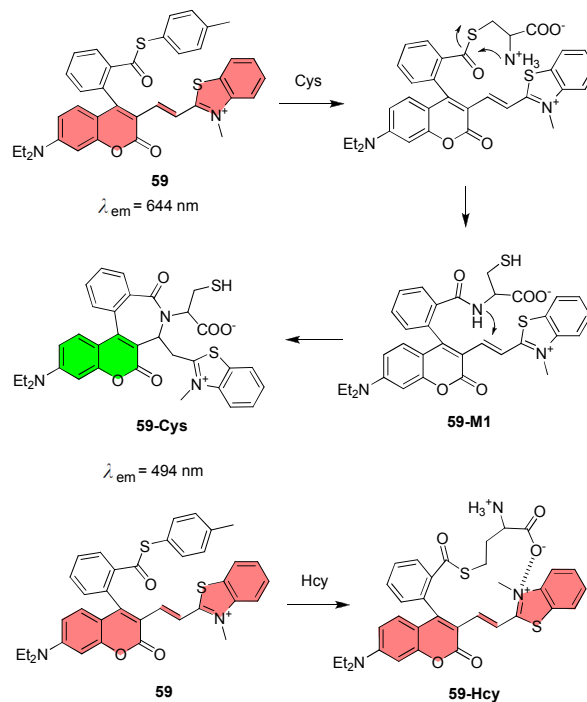


Fig. 44 Reaction of **59** with Cys and Hcy.

Probes **60-62** were designed for selective detection of GSH or Cys assisted by intramolecular hydrogen bonding. Probe **60** bears a nitroolefin moiety as the reaction site for thiols, and a *N*-phenylazacrown receptor as an additional supramolecular interaction site for recognizing GSH (Fig. 45).<sup>96</sup> In pH 6.0 (typical pH value for tumor tissues) buffered solution of **60**, addition of GSH generated stronger emission signal than addition of the equivalent amount of Cys or Hcy, presumably resulting from the interaction of ammonium group in GSH with the *N*-phenylazacrown moiety interfering with fluorescence-quenching PET. The short linker connecting the thioether and ammonium groups in Cys or Hcy adduct precludes the formation of an equivalent supramolecular complex with these thiols. Probe **60** allowed visualization of GSH distribution in the cytosol of human breast adenocarcinoma cells.

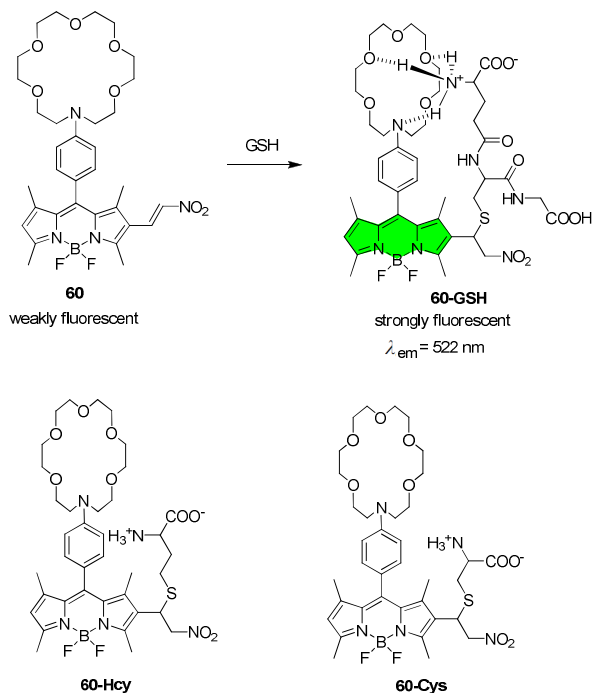


Fig. 45 The interaction of **60** with GSH vs. Cys/Hcy

Probe **61** was weakly fluorescent due to the rapid C=N isomerization in the excited state.<sup>97</sup> Upon addition of Cys/Hcy, the five-membered cyclic intramolecular hydrogen bond inhibited the C=N isomerization, leading to fluorescence enhancement. Similar strategy was utilized in Probe **62**. The Michael addition reaction between the Cys or GSH yielded **62-M1** or **62-GSH**, which were weakly fluorescent due to the C=C isomerization induced fluorescence quenching.<sup>98</sup> The intramolecular rearrangement of unstable **62-M1** led to the highly fluorescent **62-Cys**, resulting from the formation of intramolecular N-H...O hydrogen bond which inhibited the C=C bond isomerization (Fig. 46). The emission intensity of **62** at 492 nm increased linearly with Cys concentrations in the 0–30  $\mu\text{M}$  range, with the detection limit of 0.9  $\mu\text{M}$ . Probe **62** was used to selectively image Cys in human renal cells.

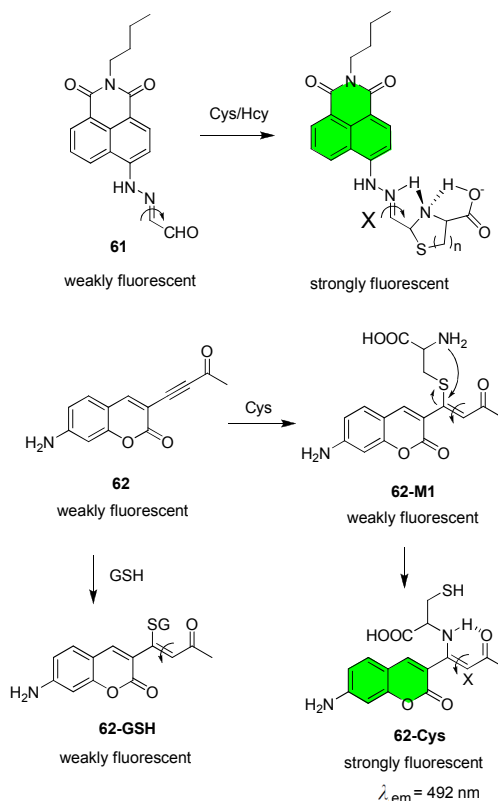


Fig. 46 The reaction of **61** and **62** with Cys/Hcy.

### 3. Conclusions

This review covers the highly topical problem of the design and studies of fluorescent probes for the selective discrimination among cysteine (Cys), homocysteine (Hcy) and glutathione (GSH). Most such probes have an electrophilic site carrying a labile substituent susceptible to nucleophilic displacement by the thiolate of these analytes or electron-poor C=C and C=O bonds susceptible to Michael addition of the S-H bond. Differentiation between GSH and Cys or Hcy exploits the propensity of aminothioethers derived from the last two thiols to undergo subsequent intramolecular rearrangement by the adjacent  $\text{NH}_2$  group to yield amino derivatives. These reactions are accompanied by changes in the absorption and/or emission maxima and/or the extinction coefficients or quantum yields of fluorescence, often enabling ratiometric detection. We classified these probes by their reaction types, including cyclization with aldehydes, conjugate addition-cyclization with acrylates, native chemical ligation and aromatic substitution-rearrangement. Integration of covalent bond-forming reactions with supramolecular interactions improved selectivity and increased reactivity of certain probes.

Despite impressive progress, challenges in designing probes for discrimination among biothiols in complex biological environment abound. For example, the probes in real biosamples containing biothiols in the mixture might suffer from the interference from each other, and other competition species (e.g. proteins with thiol groups, endogenous  $\text{H}_2\text{S}$ ) in the complex biological environment. Little effort has been investing in understanding how to exploit the high substrate selectivity of enzymes to yield highly specific probes or the

limitations that the use of enzymes may impose. Further investigation should not be restricted in the detection of Cys, Hcy and GSH, but also the thiol-containing species in specific organelles of cell or organs. Furthermore, integrating thiol targeting and imaging with strategies to deliver fluorescent probes to specific tissues and organs, as well as devising ways to localize indicators to diseased growths like tumors and plaques, may constitute an appealing approach for theranostics but await further study. Overall, the development of fluorescent probes to selectively detect thiols for bioapplications is in its infancy. Most of the commercial probes for thiols are based on Michael addition between thiols and maleimide or thiol/disulphide exchange, which cannot discriminate among thiols. We hope that this review may inspire chemists to explore new probes to selectively detect biothiols thus enabling further studies of the functions of biothiols in biological systems.



**Hai-Rong Zheng** received his B.S. degree in 2011 from Beihang University. He is currently a Ph.D. student at TIPC under the supervision of Prof. Qing-Zheng Yang. His research interests include design and synthesis of fluorescent probes and photo-responsive supramolecular assemblies.

## Biographies



**Li-Ya Niu** received both her B.S. and M.S. degrees from Beihang University (BUAA), and obtained her Ph.D. degree in organic chemistry from the Technical Institute of Physics and Chemistry, Chinese Academy of Sciences (TIPC, CAS) in 2013 under the supervision of Prof. Qing-Zheng Yang. Her research interests include the design and synthesis of fluorescent probes and their biological applications.



**Yu-Zhe Chen** obtained her Ph.D. from TIPC, CAS under the supervision of Prof. Chen-Ho Tung and Li-Zhu Wu in 2006. She then worked as a postdoctoral fellow in the group of Prof. Richard G. Weiss at Georgetown University from 2007 to 2009. She is currently an associate professor in TIPC. Her current research interests are focused on photochemistry and photophysics in supramolecular systems and optical sensors.



**Li-Zhu Wu** received her B.S. degree in chemistry from Lanzhou University in 1990, and got her Ph.D. degree from the Institute of Photographic Chemistry, CAS, under the supervision of Professor Chen-Ho Tung in 1995. From 1995–1998, she worked at the Institute of Photographic Chemistry as an associate professor. After a postdoctoral stay (1997–1998) at the University of Hong Kong working with Professor Chi-Ming Che, she returned to the TIPC, CAS, as a full professor. Her research interests are focused on photochemical conversion, including artificial photosynthesis, visible light catalysis for organic transformation, and photoinduced electron transfer, energy transfer and chemical reactions in supramolecular systems.



**Chen-Ho Tung** graduated from the polymer chemistry department of the University of Science and Technology of China in 1963, and was awarded a Ph. D. degree in 1983 from Columbia University in New York City, under the supervision of Professor Nicholas J. Turro. He joined the Institute of Photographic Chemistry, CAS, and is currently a full professor at the TIPC, and a member of the Chinese

Academy of Sciences. His research interests include photochemical reactions, photoinduced electron transfer and energy transfer in supramolecular systems.



**Qing-Zheng Yang** received his Ph.D. in 2003 from the TIPC, CAS. After completing postdoctoral research at the University Louis Pasteur and at the University of Illinois, Urbana, he returned to TIPC in 2009 as a full professor. He moved to Beijing Normal University in 2014, where he is a professor of chemistry. His research interests cover photochemistry of supramolecular assemblies and fluorescent probes for bioimaging.

### Acknowledgements

This work was financially supported by the 973 program (2013CB933800), National Natural Science Foundation of China (21222210, 21402216, 21102155) and the Fundamental Research Funds for the Central University.

### Notes and references

<sup>a</sup> Key Laboratory of Radiopharmaceuticals, Ministry of Education, College of Chemistry, Beijing Normal University, Beijing 100875, P. R. China. E-mail: qzyang@bnu.edu; Tel: +86 10 58806828

<sup>b</sup> Key Laboratory of Photochemical Conversion and Optoelectronic Materials, Technical Institute of Physics and Chemistry, Chinese Academy of Sciences, Beijing, 100190, P. R. China.

<sup>c</sup> College of Chemistry, Shandong Normal University, Jinan 250014, P.R. China.

1. S. Shahrokhian, *Anal. Chem.*, 2001, **73**, 5972-5978.
2. J. Kaluzna-Czaplinska, E. Zurawicz, M. Michalska and J. Rynkowski, *Acta Biochimica Polonica*, 2013, **60**, 137-142.
3. T. D. Dalton, H. G. Shertzer and A. Puga, *Annu. Rev. Pharmacol. Toxicol.*, 1999, **39**, 67-101.
4. A. P. de Silva, H. Q. N. Gunaratne, T. Gunnlaugsson, A. J. M. Huxley, C. P. McCoy, J. T. Rademacher and T. E. Rice, *Chem. Rev.*, 1997, **97**, 1515-1566.
5. J. Wu, W. Liu, J. Ge, H. Zhang and P. Wang, *Chemical Society Reviews*, 2011, **40**, 3483-3495.
6. M. Schaeferling, *Angew. Chem. Int. Ed.*, 2012, **51**, 3532-3554.
7. H. Kobayashi, M. Ogawa, R. Alford, P. L. Choyke and Y. Urano, *Chem. Rev.*, 2009, **110**, 2620-2640.
8. X. Li, X. Gao, W. Shi and H. Ma, *Chem. Rev.*, 2014, **114**, 590-659.
9. M. C.-L. Yeung and V. W.-W. Yam, *Chem. Soc. Rev.*, 2015. DOI: 10.1039/c4cs00391h.
10. D.-G. Cho and J. L. Sessler, *Chem. Soc. Rev.*, 2009, **38**, 1647-1662.
11. Y. Yang, Q. Zhao, W. Feng and F. Li, *Chem. Rev.*, 2013, **113**, 192-270.
12. J. Chan, S. C. Dodani and C. J. Chang, *Nat. Chem.*, 2012, **4**, 973-984.
13. X. Chen, Y. Zhou, X. Peng and J. Yoon, *Chem. Soc. Rev.*, 2010, **39**, 2120-2135.
14. H. S. Jung, X. Chen, J. S. Kim and J. Yoon, *Chem. Soc. Rev.*, 2013, **42**, 6019-6031.
15. H. Peng, W. Chen, Y. Cheng, L. Hakuna, R. Strongin and B. Wang, *Sensors*, 2012, **12**, 15907-15946.
16. T. O. Sippel, *J. of Histochem. Cytochem.*, 1981, **29**, 314-316.
17. J. V. Ros-Lis, B. Garcia, D. Jiménez, R. Martínez-Máñez, F. Sancenón, J. Soto, F. Gonzalvo and M. C. Valdecabres, *J. Am. Chem.Soc.*, 2004, **126**, 4064-4065.
18. J. Bouffard, Y. Kim, T. M. Swager, R. Weissleder and S. A. Hilderbrand, *Org. Lett.*, 2008, **10**, 37-40.
19. S. Ji, H. Guo, X. Yuan, X. Li, H. Ding, P. Gao, C. Zhao, W. Wu, W. Wu and J. Zhao, *Org. Lett.*, 2010, **12**, 2876-2879.
20. G. L. Ellman, *Arch. Biochem. Biophys.*, 1959, **82**, 70-77.
21. M. Le and G. E. Means, *Anal. Biochem.*, 1995, **229**, 264-271.
22. T. Matsumoto, Y. Urano, T. Shoda, H. Kojima and T. Nagano, *Org.Lett.*, 2007, **9**, 3375-3377.
23. B. K. McMahon and T. Gunnlaugsson, *J. Am. Chem.Soc.*, 2012, **134**, 10725-10728.
24. S. Sreejith, K. P. Divya and A. Ajayaghosh, *Angew. Chem. Int. Ed.*, 2008, **47**, 7883-7887.
25. K. Y. Law, *Chem.Rev.*, 1993, **93**, 449-486.
26. L. Yi, H. Li, L. Sun, L. Liu, C. Zhang and Z. Xi, *Angew. Chem. Int. Ed.*, 2009, **48**, 4034-4037.
27. H. Maeda, H. Matsuno, M. Ushida, K. Katayama, K. Saeki and N. Itoh, *Angew. Chem. Int. Ed.*, 2005, **44**, 2922-2925.
28. J. Zhang, A. Shibata, M. Ito, S. Shuto, Y. Ito, B. Mannervik, H. Abe and R. Morgenstern, *J. Am. Chem.Soc.*, 2011, **133**, 14109-14119.
29. J. H. Lee, C. S. Lim, Y. S. Tian, J. H. Han and B. R. Cho, *J. Am. Chem.Soc.*, 2010, **132**, 1216-1217.
30. M. H. Lee, J. H. Han, P.-S. Kwon, S. Bhuniya, J. Y. Kim, J. L. Sessler, C. Kang and J. S. Kim, *J. Am. Chem.Soc.*, 2012, **134**, 1316-1322.
31. B. Tang, Y. Xing, P. Li, N. Zhang, F. Yu and G. Yang, *J. Am. Chem.Soc.*, 2007, **129**, 11666-11667.
32. K. Xu, M. Qiang, W. Gao, R. Su, N. Li, Y. Gao, Y. Xie, F. Kong and B. Tang, *Chem. Sci.*, 2013, **4**, 1079-1086.
33. T.-K. Kim, D.-N. Lee and H.-J. Kim, *Tetrahedron Lett.*, 2008, **49**, 4879-4881.
34. X. Liu, N. Xi, S. Liu, Y. Ma, H. Yang, H. Li, J. He, Q. Zhao, F. Li and W. Huang, *J. Mater. Chem.*, 2012, **22**, 7894-7901.
35. J. Mei, Y. Wang, J. Tong, J. Wang, A. Qin, J. Z. Sun and B. Z. Tang, *Chem. -Eur. J.*, 2013, **19**, 613-620.
36. J. Mei, J. Tong, J. Wang, A. Qin, J. Z. Sun and B. Z. Tang, *J. Mater. Chem.*, 2012, **22**, 17063-17070.
37. H. Y. Lee, Y. P. Choi, S. Kim, T. Yoon, Z. Guo, S. Lee, K. M. K. Swamy, G. Kim, J. Y. Lee, I. Shin and J. Yoon, *Chem. Commun.*, 2014, **50**, 6967-6969.
38. P. Das, A. K. Mandal, N. B. Chandar, M. Baidya, H. B. Bhatt, B. Ganguly, S. K. Ghosh and A. Das, *Chem. -Eur. J.*, 2012, **18**, 15382-15393.

39. O. Rusin, N. N. St Luce, R. A. Agbaria, J. O. Escobedo, S. Jiang, I. M. Warner, F. B. Dawan, K. Lian and R. M. Strongin, *J. Am. Chem. Soc.*, 2004, **126**, 438-439.
40. W. Lin, L. Long, L. Yuan, Z. Cao, B. Chen and W. Tan, *Org. Lett.*, 2008, **10**, 5577-5580.
41. K.-S. Lee, T.-K. Kim, J. H. Lee, H.-J. Kim and J.-I. Hong, *Chem. Commun.*, 2008, 6173-6175.
42. J. Zhang, X.-D. Jiang, X. Shao, J. Zhao, Y. Su, D. Xi, H. Yu, S. Yue, L.-j. Xiao and W. Zhao, *Rsc Advances*, 2014, **4**, 54080-54083.
43. L. Duan, Y. Xu, X. Qian, F. Wang, J. Liu and T. Cheng, *Tetrahedron Lett.*, 2008, **49**, 6624-6627.
44. Z. Yang, N. Zhao, Y. Sun, F. Miao, Y. Liu, X. Liu, Y. Zhang, W. Ai, G. Song, X. Shen, X. Yu, J. Sun and W.-Y. Wong, *Chem. Commun.*, 2012, **48**, 3442-3444.
45. Y. Ma, S. Liu, H. Yang, Y. Wu, C. Yang, X. Liu, Q. Zhao, H. Wu, J. Liang, F. Li and W. Huang, *J. Mater. Chem.*, 2011, **21**, 18974-18982.
46. W. H. Wang, O. Rusin, X. Y. Xu, K. K. Kim, J. O. Escobedo, S. O. Fakayode, K. A. Fletcher, M. Lowry, C. M. Schowalter, C. M. Lawrence, F. R. Fronczek, I. M. Warner and R. M. Strongin, *J. Am. Chem. Soc.*, 2005, **127**, 15949-15958.
47. H. Li, J. Fan, J. Wang, M. Tian, J. Du, S. Sun, P. Sun and X. Peng, *Chem. Commun.*, 2009, 5904-5906.
48. L. Yuan, W. Lin and Y. Yang, *Chem. Commun.*, 2011, **47**, 6275-6277.
49. S. Madhu, R. Gonnade and M. Ravikanth, *Journal of Organic Chemistry*, 2013, **78**, 5056-5060.
50. F. Guo, M. Tian, F. Miao, W. Zhang, G. Song, Y. Liu, X. Yu, J. Z. Sun and W.-Y. Wong, *Org. Biomol. Chem.*, 2013, **11**, 7721-7728.
51. H. Chen, Q. Zhao, Y. Wu, F. Li, H. Yang, T. Yi and C. Huang, *Inorg. Chem.*, 2007, **46**, 11075-11081.
52. A. Barve, M. Lowry, J. O. Escobedo, K. T. Huynh, L. Hakuna and R. M. Strongin, *Chem. Commun.*, 2014, **50**, 8219-8222.
53. W. Wang, J. O. Escobedo, C. M. Lawrence and R. M. Strongin, *J. Am. Chem. Soc.*, 2004, **126**, 3400-3401.
54. J. O. Escobedo, W. Wang and R. M. Strongin, *Nat. Protocols*, 2006, **1**, 2759-2762.
55. L. Hakuna, J. O. Escobedo, M. Lowry, A. Barve, N. McCallum and R. M. Strongin, *Chem. Commun.*, 2014, **50**, 3071-3073.
56. X. Yang, Y. Guo and R. M. Strongin, *Angew. Chem. Int. Ed.*, 2011, **50**, 10690-10693.
57. B. Liu, J. Wang, G. Zhang, R. Bai and Y. Pang, *ACS Appl. Mater. Inter.*, 2014, **6**, 4402-4407.
58. H. Wang, G. Zhou, H. Gai and X. Chen, *Chem. Commun.*, 2012, **48**, 8341-8343.
59. X. Yang, Y. Guo and R. M. Strongin, *Org. Biomol. Chem.*, 2012, **10**, 2739-2741.
60. X. Dai, Q.-H. Wu, P.-C. Wang, J. Tian, Y. Xu, S.-Q. Wang, J.-Y. Miao and B.-X. Zhao, *Biosens. Bioelectron.*, 2014, **59**, 35-39.
61. B. Zhu, B. Guo, Y. Zhao, B. Zhang and B. Du, *Biosens. Bioelectron.*, 2014, **55**, 72-75.
62. Q. Han, Z. Shi, X. Tang, L. Yang, Z. Mou, J. Li, J. Shi, C. Chen, W. Liu, H. Yang and W. Liu, *Org. Biomol. Chem.*, 2014, **12**, 5023-5030.
63. Z. Guo, S. Nam, S. Park and J. Yoon, *Chem. Sci.*, 2012, **3**, 2760-2765.
64. B. Zhu, Y. Zhao, Q. Zhou, B. Zhang, L. Liu, B. Du and X. Zhang, *Chem. -Eur. J.*, 2013, 888-893.
65. K.-H. Hong, S.-Y. Lim, M.-Y. Yun, J.-W. Lim, J.-H. Woo, H. Kwon and H.-J. Kim, *Tetrahedron Lett.*, 2013, **54**, 3003-3006.
66. D. P. Murale, H. Kim, W. S. Choi and D. G. Churchill, *RSC Adv.*, 2014, **4**, 5289-5292.
67. S.-Q. Wang, Q.-H. Wu, H.-Y. Wang, X.-X. Zheng, S.-L. Shen, Y.-R. Zhang, J.-Y. Miao and B.-X. Zhao, *Biosens. Bioelectron.*, 2014, **55**, 386-390.
68. Q. Zhang, D. Yu, S. Ding and G. Feng, *Chem. Commun.*, 2014, **50**, 14002-14005.
69. Y. Guo, X. Yang, L. Hakuna, A. Barve, J. O. Escobedo, M. Lowry and R. M. Strongin, *Sensors*, 2012, **12**, 5940-5950.
70. L. Wei, A. Lucas, J. Yue and R. B. Lennox, *Langmuir*, 1991, **7**, 1336-1339.
71. L. Wang, H. Chen, H. Wang, F. Wang, S. Kambam, Y. Wang, W. Zhao and X. Chen, *Sensor Actuat. B-Chem.*, 2014, **192**, 708-713.
72. A. Agostini, I. Campos, M. Milani, S. Elsayed, L. Pascual, R. Martinez-Manez, M. Licchelli and F. Sancenon, *Org. Biomol. Chem.*, 2014, **12**, 1871-1874.
73. L. Long, W. Lin, B. Chen, W. Gao and L. Yuan, *Chem. Commun.*, 2011, **47**, 893-895.
74. L. Yuan, W. Lin, Y. Xie, S. Zhu and S. Zhao, *Chem. -Eur. J.*, 2012, **18**, 14520-14526.
75. E. C. B. Johnson and S. B. H. Kent, *J. Am. Chem. Soc.*, 2006, **128**, 6640-6646.
76. X.-F. Yang, Q. Huang, Y. Zhong, Z. Li, H. Li, M. Lowry, J. O. Escobedo and R. M. Strongin, *Chem. Sci.*, 2014, **5**, 2177-2183.
77. L.-Y. Niu, Y.-S. Guan, Y.-Z. Chen, L.-Z. Wu, C.-H. Tung and Q.-Z. Yang, *J. Am. Chem. Soc.*, 2012, **134**, 18928-18931.
78. L.-Y. Niu, Q.-Q. Yang, H.-R. Zheng, Y.-Z. Chen, L.-Z. Wu, C.-H. Tung and Q.-Z. Yang, *Rsc Adv.*, 2015, **5**, 3959-3964.
79. F. Wang, Z. Guo, X. Li, X. Li and C. Zhao, *Chem. -Eur. J.*, 2014, **20**, 11471-11478.
80. D. H. Ma, D. Kim, E. Seo, S.-J. Lee and K. H. Ahn, *Analyst*, 2015, **140**, 422-427.
81. L.-Y. Niu, H.-R. Zheng, Y.-Z. Chen, L.-Z. Wu, C.-H. Tung and Q.-Z. Yang, *Analyst*, 2014, **139**, 1389-1395.
82. M. D. Hammers and M. D. Pluth, *Anal. Chem.*, 2014, **86**, 7135-7140.
83. X. Wang, J. Lv, X. Yao, Y. Li, F. Huang, M. Li, J. Yang, X. Ruan and B. Tang, *Chem. Commun.*, 2014, **50**, 15439-15442.
84. Y.-S. Guan, L.-Y. Niu, Y.-Z. Chen, L.-Z. Wu, C.-H. Tung and Q.-Z. Yang, *Rsc Advances*, 2014, **4**, 8360-8364.
85. S.-Y. Lim, K.-H. Hong, D. I. Kim, H. Kwon and H.-J. Kim, *J. Am. Chem. Soc.*, 2014, **136**, 7018-7025.
86. L. Ma, J. Qian, H. Tian, M. Lan and W. Zhang, *Analyst*, 2012, **137**, 5046-5050.
87. L. Song, T. Jia, W. Lu, N. Jia, W. Zhang and J. Qian, *Org. Biomol. Chem.*, 2014, **12**, 8422-8427.
88. J. Liu, Y.-Q. Sun, H. Zhang, Y. Huo, Y. Shi and W. Guo, *Chem. Sci.*, 2014, **5**, 3183-3188.
89. J. Liu, Y.-Q. Sun, Y. Huo, H. Zhang, L. Wang, P. Zhang, D. Song, Y. Shi and W. Guo, *J. Am. Chem. Soc.*, 2014, **136**, 574-577.
90. N. Shao, J. Y. Jin, S. M. Cheung, R. H. Yang, W. H. Chan and T. Mo, *Angew. Chem. Int. Ed.*, 2006, **45**, 4944-4948.
91. N. Shao, J. Jin, H. Wang, J. Zheng, R. Yang, W. Chan and Z. Abliz, *J. Am. Chem. Soc.*, 2010, **132**, 725-736.

## Journal Name

92. Y. Li, Y. Duan, J. Li, J. Zheng, H. Yu and R. Yang, *Anal. Chem.*, 2012, **84**, 4732-4738.
93. X. Zhou, X. Jin, G. Sun, D. Li and X. Wu, *Chem. Commun.*, 2012, **48**, 8793-8795.
94. X. Zhou, X. Jin, G. Sun and X. Wu, *Chem. – Eur. J.*, 2013, **19**, 7817-7824.
95. J. Liu, Y.-Q. Sun, H. Zhang, Y. Huo, Y. Shi, H. Shi and W. Guo, *Rsc Adv.*, 2014, **4**, 64542-64550.
96. M. Isik, R. Guliyev, S. Kolemen, Y. Altay, B. Senturk, T. Tekinay and E. U. Akkaya, *Org. Lett.*, 2014, **16**, 3260-3263.
97. P. Wang, J. Liu, X. Lv, Y. Liu, Y. Zhao and W. Guo, *Org. Lett.*, 2012, **14**, 520-523.
98. Y. Liu, S. Zhang, X. Lv, Y.-Q. Sun, J. Liu and W. Guo, *Analyst*, 2014, **139**, 4081-4087.